Journal of Cardiovascular
Magnetic Resonance

REVIEW Open Access

CrossMark

Review of Journal of Cardiovascular Magnetic Resonance (JCMR) 2015-2016 and transition of the JCMR office to Boston

Warren J. Manning

Abstract

The *Journal of Cardiovascular Magnetic Resonance (JCMR)* is the official publication of the Society for Cardiovascular Magnetic Resonance (SCMR). In 2016, the *JCMR published* 93 manuscripts, including 80 research papers, 6 reviews, 5 technical notes, 1 protocol, and 1 case report. The number of manuscripts published was similar to 2015 though with a 12% increase in manuscript submissions to an all-time high of 369. This reflects a decrease in the overall acceptance rate to <25% (excluding solicited reviews). The quality of submissions to JCMR continues to be high. The 2016 *JCMR* Impact Factor (which is published in June 2016 by Thomson Reuters) was steady at 5.601 (vs. 5.71 for 2015; as published in June 2016), which is the second highest impact factor ever recorded for *JCMR*. The 2016 impact factor means that the *JCMR* papers that were published in 2014 and 2015 were on-average cited 5.71 times in 2016.

In accordance with Open-Access publishing of Biomed Central, the *JCMR* articles are published on-line in the order that they are accepted with no collating of the articles into sections or special thematic issues. For this reason, over the years, the Editors have felt that it is useful to annually summarize the publications into broad areas of interest or themes, so that readers can view areas of interest in a single article in relation to each other and other recent *JCMR* articles. The papers are presented in broad themes with previously published *JCMR* papers to guide continuity of thought in the journal. In addition, I have elected to open this publication with information for the readership regarding the transition of the *JCMR* editorial office to the Beth Israel Deaconess Medical Center, Boston and the editorial process.

Though there is an author publication charge (APC) associated with open-access to cover the publisher's expenses, this format provides a much wider distribution/availability of the author's work and greater manuscript citation. For SCMR members, there is a substantial discount in the APC. I hope that you will continue to send your high quality manuscripts to *JCMR* for consideration. Importantly, I also ask that you consider referencing recent *JCMR* publications in your submissions to the *JCMR* and elsewhere as these contribute to our impact factor. I also thank our dedicated Associate Editors, Guest Editors, and reviewers for their many efforts to ensure that the review process occurs in a timely and responsible manner and that the *JCMR* continues to be recognized as the leading publication in our field.

JCMR transition to Boston/editorial process

At the end of December 2016, the editorial office of the Journal of Cardiovascular Magnetic Resonance (*JCMR*) moved to the Beth Israel Deaconess Medical Center, Boston under the leadership of Dr. Warren J. Manning – former Deputy Editor of the *JCMR* and current editor-in-chief. Manuscripts that were in processing at the Royal Brompton Hospital *JCMR* office continued to be handled by that office and all *JCMR* activities under

Dr. Pennell's leadership and editorial team ceased at the end of April 2017.

JCMR leadership/communication

As compared with the prior two editor's handling of all editor/associate editor activities at their "home" institution, the current *JCMR* Associate Editors are diverse in geography and include (Fig. 1) Drs. Rene Botnar (Kings College, London, UK/Chile), John Greenwood (University of Leeds, UK), Yuchi Han (University of Pennsylvania Health System, USA), Dara Kraitchman (Johns Hopkins University School of Medicine, USA),

Correspondence: wmanning@bidmc.harvard.edu; jcmreditor@scmr.org
From the Journal of Cardiovascular Magnetic Resonance Editorial Office and the Beth Israel Deaconess Medical Center, Harvard Medical School, Boston, MA, USA

Fig. 1 2017 *JCMR* Editorial team
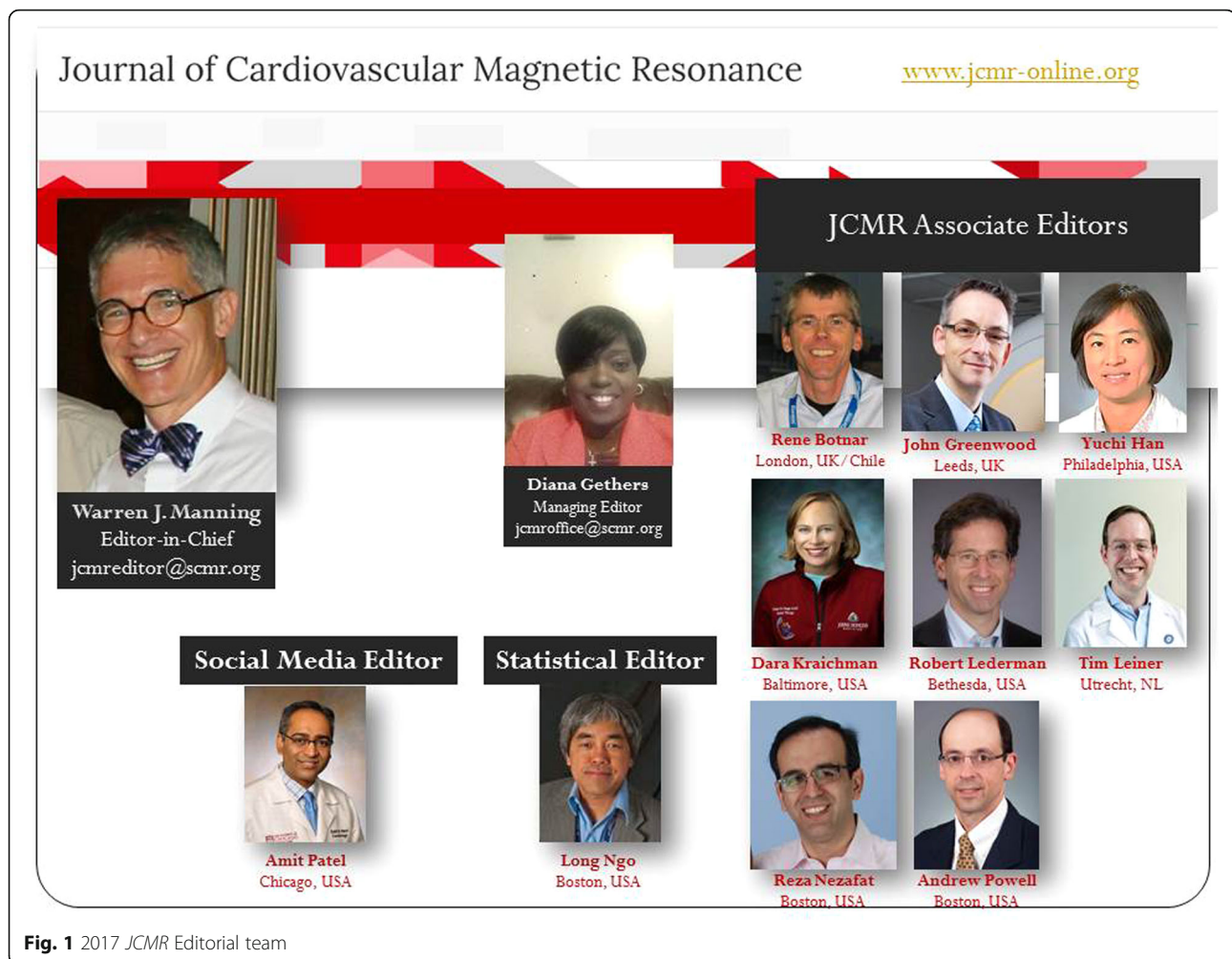
Robert Lederman (National Heart, Lung, and Blood Institute, USA), Tim Leiner (UMC Utrecht, The Netherlands), Reza Nezafat (Beth Israel Deaconess Medical Center/Harvard Medical School, USA) and Andrew Powell (Children's Hospital Boston/Harvard Medical School, USA). In addition, Dr. Long Ngo (Beth Israel Deaconess Medical Center/Harvard Medical School, USA) serves as the *JCMR* statistical editor and Dr. Amit Patel (University of Chicago, USA) serves as our social media editor. Ms. Gifty Addae served as our managing editor until August 2017, after which Mrs. Diana Gethers took on the responsibilities as our managing editor. Despite the change in managing editor leadership, the *JCMR* office email address continues to be jcmroffice@scmr.org.

To facilitate communication in an era of constant change, a generic email address between the *JCMR* and readership was instituted including the use of **jcmreditor@scmr.org** for the editor-in-chief and **jcmroffice@scmr.org** for the managing editor.

JCMR publication/review process

The *JCMR* is the official publication of the Society for Cardiovascular Magnetic Resonance (SCMR) and has been published in open access format for a decade through BioMed Central (BMC) as the publisher. All manuscripts are submitted through the www.jcmr-online.biomedcentral.com website.

After initial confirmation that the manuscript is in the appropriate format (abstract, text, references, figures, tables, etc.) by the BMC office, the manuscript is sent for initial review to the Boston editorial office. Within 48 h, the manuscript is assessed for its appropriateness for the *JCMR* readership and a determination as to its overall likely priority for publication. Approximately 20% of submitted manuscripts are returned to the author at this stage and without review so as to expedite their submission to another more appropriate journal. Authors are often offered the opportunity to submit their work to another BMC open access publication. Nearly 50% of authors take advantage of this option.

Reviewer assignments are then requested for manuscripts that are deemed worthy of further review and the manuscript is assigned to one of our Associate Editors. Reviews are requested within 2 weeks and reviewers are asked to follow specific submission guidelines as outlined in their offer letter. We are fortunate to have over 1162 registered reviewers, but are continually looking to expand our reviewer pool, engaging younger members/innovators of the CMR field. If you are interested in becoming a *JCMR* reviewer, please sign up to be a reviewer at **https://www.surveymonkey.com/r/JCMRreview** or contact our managing editor, Diana Gethers [jcmroffice@scmr.org].

When at least two reviews have been received, the Associate Editor presents the manuscript at our Web-Ex Associate Editorial board meeting held every Tuesday morning from 9:30-10:30 am EST. [When I am out of town/away, the Associate Editors continue to meet at that time so as to not delay the publication process.] At each meeting, 4-12 manuscripts may be discussed. Decisions include

1) Accept
2) Minor revision – no new experiments are needed, relatively minor text changes or analysis requested, 30 day turn-around; >98% acceptance is anticipated
3) Major revision – substantial text and or analysis needed, a few experiments; 90 day turn-around; ~60% acceptance is anticipated
4) De novo resubmission – substantial new experiments/analysis are needed; unlimited turn-around; ~35% acceptance is anticipated
5) Decline/reject

Our target goal is than 60% of manuscripts will have a submission to *first* decision within 31 days, a process that is very dependent on our receipt of timely reviews. If the two reviews markedly differ in their assessment (~25% of the time), a third reviewer is often solicited – a process than can add up to a month to the overall review process. In rare instances, a fourth review may be requested. When added reviews are requested, we try to alert the corresponding author that there will be a delay. Revisions may (major some minor) or may not (most minor) be sent to the prior or new reviewers. Denovo resubmissions are usually sent to the original manuscript reviewers.

Conflicts of interest

Rather than having a single deputy editor to handle "conflict of interest "manuscripts submitted by members of the Associate Editorial team (or their close associates), these manuscripts are handled by a Guest Editor. The activities of the Guest Editor are conducted outside/independent of the Boston editorial office. If accepted, the Guest Editor is disclosed in the publication.

Social media

Initiated by our formed editor-in-chief, Professor Dudley Pennell, the *JCMR* is active on Twitter with the handle "**JournalofCMR**". This relationship is coordinated by Dr. Amit Patel. As of mid-November 2016, our Twitter statistics indicate that we have 990 followers and have had 153,070 total impressions; 6848 engagements, 723 retweets, 1629 URL clicks, and 2377 media views. In 2017, our engagement rate has increased from 1.30 to 1.51.

Continuing medical education

New for 2017 is our development of a process for our readership to receive Continuing Medical Education (CME) credit for *JCMR* publications through the SCMR. Ongoing level II/III certification in CMR requires CME credit. The first CME offering was for a manuscript by Chan and colleagues on the tissue characterization of cardiac neoplasm and thrombus [1]. We had 2 offerings in 2017 and hope to have quarterly offerings in 2018. In 2018, we also hope to offer CME credit for our reviewers. Stay tuned!

Gerald M. Pohost award/Dudley Pennell award

For the past decade, the SCMR has presented the Gerald M. Pohost Award to that manuscript identified by the *JCMR* editorial board to be *the most important JCMR publication* of the prior year. Dr. Pohost was the first *JCMR* editor-in-chief. The 2017 Gerald M. Pohost Award was presented to Dr. Shazia Hussain and colleagues for their publication "Perfusion cardiovascular magnetic resonance and fractional flow reserve in patients with angiographic multi-vessel coronary artery disease." [2][Fig. 2]. Beginning with the 2018 SCMR Annual Meeting, in recognition to our 2nd editor-in-chief and the tremendous rise in the *JCMR* Impact Factor during his tenure, we will also be presenting the inaugural Dudley Pennell Award to that original research

Fig. 2 The 2017 Gerald M. Pohost Award is presented at the 2017 annual meeting of the SCMR

manuscript which has received the highest number of citations (thereby contributing to the *JCMR* impact factor) for the calendar year 3 years prior to the award (i.e, 2018 Dudley Pennell Prize will be awarded to that original research manuscript published in calendar year 2014).

2016 Publications:

Listed below are summaries of the 2015/2016 *JCMR* publications presented in thematic format with the reference (2015 publications) [3] and brief manuscript synopsis (2016 publications).

Cardiomyopathies

Cardiac phenotyping continues to be a primary clinical indication for CMR, and has become mainstream in the common cardiomyopathies including hypertrophic cardiomyopathy (HCM; [4, 5]), Anderson-Fabry Disease [6, 7], dilated cardiomyopathy [8–11], left ventricular non-compaction (LVNC [12], myocarditis [13–16], Chagas disease [17], cardiac siderosis [18] and right ventricular dysfunction due to pulmonary hypertension [19, 20].

Hypertrophic cardiomyopathy
Microvascular ischemia in hypertrophic cardiomyopathy: new insights from high-resolution combined quantification of perfusion and late gadolinium enhancement.

Microvascular ischemia is one of the hallmarks of hypertrophic cardiomyopathy (HCM) and has been associated with poor outcomes. Villa and co-workers [21] examined 30 HCM patients with non-obstructive epicardial coronary arteries with Fermi constrained quantitative perfusion analysis on segmental and high-resolution data. High resolution quantification proved to be more sensitive for the detection of microvascular ischemia in comparison with segmental analysis. Areas of late gadolinium enhancement (LGE) were associated with a significant reduction in myocardial perfusion reserve (MPR) leading to an *overestimation* of the total ischemic burden. Using an MPR of 1.5, the presence of LGE was found to lead to an ischemic burden overestimation of 28%.

Cardiovascular magnetic resonance of mitral valve length in hypertrophic cardiomyopathy.

Prior data suggest that mitral leaflet elongation in hypertrophic cardiomyopathy (HCM). Tarkiainen et al. [22] studied 47 HCM subjects with Q1061X mutation in the gene encoding MYBPC3 and 20 relatives without the mutation. Subjects with the MYBPC3-Q1061X mutation included 32 with left ventricular (LV) hypertrophy. The absolute posterior mitral leaflets was longer in the MYBPC3-Q1061X patients, but was not significant when the posterior leaflet length was indexed for body surface area. There was no difference in posterior mitral leaflet length in mutations carriers without LV hypertrophy and healthy controls.

Anderson-Fabry disease
Cardiovascular magnetic resonance demonstration of the spectrum of morphological phenotypes and patterns of myocardial scarring in Anderson-Fabry disease.

Anderson-Fabry disease can mimic hypertrophic cardiomyopathy (HCM) on transthoracic echocardiography. Deva and co-workers [23] studied 39 Anderson-Fabry patients (20 M) and found that 44% had concentric wall thickening. In addition, 44% had pathologic scar/late gadolinium enhancement (LGE) of which 76% had typical inferolateral midwall LGE. Patients with elevated left ventricular (LV) mass index had more ventricular arrhythmia and sustained ventricular tachycardia.

Amyloid Cardiomyopathy
Regional myocardial microvascular dysfunction in cardiac amyloid light-chain amyloidosis: assessment with 3T cardiovascular magnetic resonance.

Coronary microvascular dysfunction is highly prevalent in patients with cardiac light-chain (AL) amyloidosis. In this study by Li and co-workers [24] performed regional myocardial perfusion CMR in 32 patients with biopsy proven cardiac AL amyloidosis and systolic dysfunction, 21 patients with cardiac AL amyloidosis and preserved systolic function, and 25 healthy subjects. Patients with cardiac AL amyloidosis had significantly reduced first pass perfusion upslope and maximal signal intensity. Compared with cardiac AL amyloid patients with preserved systolic function, those with depressed systolic function has a longer time to maximum signal intensity in the basal and mid-ventricular segments and lower upslope in the basal, mid, and apical segments.

Non-ischemic cardiomyopathies:
Mechanical effects of left ventricular midwall fibrosis in non-ischemic cardiomyopathy.

Left ventricular mid-wall fibrosis occurs in a quarter of patients with a non-ischemic cardiomyopathy and is associated with high risk of pump failure. Taylor and colleagues [25] examined 116 patients who underwent late gadolinium enhancement (LGE) CMR with feature tracking CMR to assess myocardial deformation. Despite similar left ventricular ejection fraction (LVEF), patients with mid-wall fibrosis had lower global circumferential strain, strain rate, and torsion, but similar longitudinal and radial strain.

Analyzing myocardial torsion based on tissue phase mapping cardiovascular magnetic resonance.

Chitiboi et al. [26] performed tissue phase mapping (base, mid, apical short axis) and late gadolinium enhancement (LGE) in 27 patients with non-ischemic cardiomyopathy and tissue phase mapping in 14 healthy subjects. Maximal myocardial torsion was significantly lower for the cardiomyopathic patients. Global myocardial torsion showed a positive correlation with left ventricular (LV) ejection fraction (LVEF). Moreover, endocardial torsion was significantly higher than epicardial torsion for normal LVEF subjects.

Relationship between native papillary muscle T1 time and severity of functional mitral regurgitation in patients with non-ischemic dilated cardiomyopathy.

Functional mitral regurgitation is one of the severe complications of non-ischemic dilated cardiomyopathy. Kato and co-workers [27] studied 40 patients with non-ischemic cardiomyopathy and 20 healthy controls and found both papillary muscle native T1 were significantly elevated in the cardiomyopathy group with mitral regurgitation v. those without mitral regurgitation. Multivariate linear regression analysis showed that papillary muscle native T1 correlated with mitral regurgitant fraction. Elevated papillary muscle native T1 was also associated with larger diameter, longer length, and decreased papillary muscle shortening.

Objective criteria for septal fibrosis in non-ischemic dilated cardiomyopathy: validation for the prediction of future cardiovascular events.

Expert subjective mid-wall septal fibrosis on late gadolinium enhancement (LGE) CM R has been shown to predict major adverse cardiovascular outcomes. Mikami et al. [28] sought to establish objective criteria for non-experts and studied 118 consecutive patients with a non-ischemic cardiomyopathy and septal fibrosis identified by an expert reader. CMR naïve readers performed signal threshold-based LGE quantification. At nearly 2 year follow-up, 17% of patients had a primary composite outcome. Expert visual scoring identified 55 patients with septal fibrosis. Receiver operator curve analysis demonstrated the optimal threshold for prediction of primary outcome were 5SD; a level that also was the strongest independent predictor of the primary outcome and provided improved risk reclassification beyond left ventricular ejection fraction (LVEF).

Muscular dystrophies
Increased myocardial native T1 and extracellular volume in patients with Duchenne muscular dystrophy.

Duchenne's muscular dystrophy cardiomyopathy is a progressive incurable disorder. Detection of subclinical disease may be useful for early intervention and for monitoring disease specific therapies. In this prospective study, Soslow and colleagues [29] examined native T1 and extracellular volume fraction (ECV) in 31 Duchenne's patients and 11 healthy controls. They found that even in the Duchenne's subset with a normal left ventricular ejection fraction (LVEF) and no late gadolinium enhancement (LGE), Duchenne participants had a greater native T1 and greater ECV.

Identification of cardiomyopathy associated circulating miRNA biomarkers in patients with muscular dystrophy using a complementary cardiovascular magnetic resonance and plasma profiling approach.

Duchenne and Becker muscular dystrophy are x-linked recessive neuromuscular disorders. In this study, Becker et al. [30] prospectively examined 63 male patients with known muscular dystrophy and 26 age-matched healthy controls. Impaired left ventricular (LV) systolic function (ejection fraction <55%) and a non-ischemic late gadolinium enhancement (LGE) pattern were found in 46% and 76% of muscular dystrophy patients, respectively. A significant upregulation of circulating miRNAs miR-222, miR-26a, and miR-378-5p were independent predictors for LGE.

Myocardial late gadolinium enhancement is associated with clinical presentation in Duchenne muscular dystrophy.

Duchenne's muscular dystrophy is an x-linked recessive disease that occurs in males leading to immobility and death in early adulthood. Female carriers are generally asymptomatic, but sometimes develop a dilated cardiomyopathy. Wexberg and colleagues [31] studied 20 Duchenne's carriers, the majority of which (90%) were asymptomatic, yet nearly half had late gadolinium enhancement (LGE), all of whom were NYHA class II or III. LGE positive carriers had lower left ventricular (LV) ejection fraction, higher creatine phosphokinase and shorter 6-min walk test.

Native T1 values identify myocardial changes and disease severity in patients with Duchenne muscular dystrophy.

Duchenne's muscular dystrophy is an x-linked, inherited disorder that leads to a dilated cardiomyopathy with variable onset and progression. Olivieri and co-workers [32] examined 20 boys with Duchenne's and 16 age and gender matched controls and found 60% of the Duchenne subjects and late gadolinium enhancement (LGE) of the lateral wall. Native T1 and extracellular volume fraction (ECV) were also significantly higher in the Duchenne cohort with both MOLLI and SASHA T1 sequences. ECV demonstrated the ability to predict the

presence of LGE, but could not distinguish between healthy controls and Duchenne's without LGE.

Left ventricular non-compaction
Quantification of left ventricular trabeculae using cardiovascular magnetic resonance for the diagnosis of left ventricular non-compaction: evaluation of trabecular volume and refined semi-quantitative criteria.

There is no consensus for the diagnosis of left ventricular non-compaction (LVNC). In this study Choi and co-workers [33] retrospectively identified 145 subjects with mild to severe left ventricular (LV) trabeculations, 24 patients with isolated LVNC, 33 patients with non-isolated LVNC, and 30 patients with dilated cardiomyopathy. The patients with isolated LVNC had trabecular LV volume that was 1.4× greater than those with a dilated cardiomyopathy and 1.7× greater than the healthy controls. There was no difference in the percent trabecular volume between the isolated LVNC and dilated cardiomyopathy groups. A percent trabecular volume threshold of >34.6% had a specificity of 89.7% and sensitivity of 66.1% for LVNC.

Chagas disease
Chagas' heart disease: gender differences in myocardial damage assessed by cardiovascular magnetic resonance.

A male-related higher incidence of cardiovascular morbidity and mortality has been described with Chagas heart disease. Assunacao and colleagues [34] retrospectively identified 62 seropositive Chagas' heart disease patients and low probability of coronary artery disease (CAD) referred for CMR at 1.5T. There was a strong correlation between left ventricular (LV) ejection fraction (LVEF) and late gadolinium enhancement (LGE) with men showing greater LGE (including transmural pattern) and lower LVEF. After adjustment for confounders, male gender remained associated with LV dysfunction with 5% of the effect mediated by LGE.

Pompe disease
Pattern and prognostic value of cardiac involvement in patients with late-onset Pompe Disease: a comprehensive cardiovascular magnetic resonance approach.

Pompe disease is an autosomal recessive disorder caused by a deficiency of the lysosomal alpha-1,4-glucosidase which leads to an accumulation of glycogen in target tissue and progressive organ failure. Boentert and co-workers [35] studied 17 patients with genetically proven late-onset Pompe disease (50 +/− 18 years; 11 men) and 18 age and gender matched controls with CMR. They found that all Pompe Disease patients had normal left ventricular (LV) and right ventricular (RV) volumes and ejection fraction and feature tracking measures of left ventricular strain. Three (18%) of the Pompe Disease patients had a non-ischemic late gadolinium enhancement (LGE) pattern and 21% had an elevated extracellular volume fraction (ECV).

Obesity
Cardiac remodeling and dysfunction in childhood obesity: a cardiovascular magnetic resonance study.

Obesity affects nearly 20% of children and is associated with an increased premature death. In this study, Jing and colleagues [36] performed CMR in 41 obese/overweight and 29 healthy weight children. After adjusting for age, LV mass index was 23% greater and the myocardial wall was 10-% thicker in the obese/overweight cohort. Nearly a quarter of the obese/overweight cohort had concentric hypertrophy. Peak longitudinal strain and circumferential strain showed a significant relationship with the type of remodeling and were most impaired in children with concentric hypertrophy.

Connective tissue disorders
Evaluation of myocardial involvement in patients with connective tissue disorders: a multi-parametric cardiovascular magnetic resonance study.

Arrhythmias and heart failure are sometimes found in patients with connective tissue disorders and myocardial involvement. Mayr and co-workers [37] prospectively performed CMR in 40 patients with connective tissue disorder and 20 healthy controls. They found that 18% of connective tissue disorder sometimes displayed late gadolinium enhancement (LGE). The connective tissue disorder group also had a greater extracellular volume (ECV), T2, and native T1 with lower post-contrast T1.

Cardiovascular magnetic resonance patterns of biopsy proven cardiac involvement in systemic sclerosis.

Systemic sclerosis may sometimes involve the myocardium. In this retrospective study, Krumm et al. [38] identified 20 patients with biopsy proved cardiac involvement in systemic sclerosis and found 45% had a moderate (>5 mm) or greater pericardial effusion; 95% had reduced left ventricular (LV) or right ventricular (RV) systolic function and 70% of patients had late gadolinium enhancement (LGE). Seven (35%) of patients had all three categories of abnormalities.

Arrhythmogenic right ventricular cardiomyopathy
Ventricular structure in ARVC: going beyond volumes as a measure of risk.

Altered right ventricular (RV) anatomy and function is an important feature of the arrhythmogenic right ventricular cardiomyopathy (ARVC) phenotype. In this retrospective, cross-sectional study, McLeod and co-

workers [39] examined CMR short axis cines in 27 ARVC patients and 21 asymptomatic control subjects. They found that the ARVC cohort was more likely to have global dilation/shrinking of both ventricles (44%), elongation/shortening of the RV (15%), tilting of the septum (10%), shortening/lengthening of both ventricles (7%), and bulging/shortening of both the RV inflow and outflow (5%). Classification of ARVC v. controls using shape modes had a sensitivity and specificity of 96% and 81%, respectively.

Syndrome X
Coronary microvascular function and myocardial fibrosis in women with angina pectoris and no obstructive coronary artery disease: the iPOWER study.

Despite the absence of obstructive coronary artery disease, women with angina pectoris have a poor prognosis due to microvascular disease. Mygind et al. [40] performed CMR and coronary flow velocity reserve in 64 women with angina a no obstructive coronary artery disease. None had focal late gadolinium enhancement. No significant correlations were found between coronary flow velocity reserve and extracellular volume fraction (ECV) or native T1. In addition, no relationship was seen between myocardial blood flow reserve and ECV or native T1.

Cost Effectiveness/Databases/Normative Values.

With the increasing focus on the growing societal burden of health care costs, it is imperative that CMR demonstrate safety [41], value/cost effectiveness/appropriateness [42, 43]. Increasing large databases to define normative CMR parameters [44–49] are also reported.

Cost effectiveness
Cost-minimization analysis of three decision strategies for cardiac revascularization: results of the "suspected CAD" cohort of the European Cardiovascular Magnetic Resonance Registry.

Coronary artery disease (CAD) continues to be the leading cause of morbidity and mortality in the developed world. While perfusion CMR is generally accepted as clinically useful, cost-effectiveness data are scarce. Moschetti et al. [50] examined 3647 patients with suspected CAD from the European Cardiovascular Magnetic Resonance Registry and examined costs over a 1 year period for CMR, x-ray angiography with/without fractional flow reserve, revascularization, and complications. Coronary revascularization was performed in 6.2% of the entire group, including 4.5% and 12.9% of those with atypical and typical chest pain, respectively. A CMR + xray angiography strategy reduced costs by 14-34% vs. x-ray angiography + fractional flow reserve strategy and by >50% when compared with x-ray angiography only strategy.

CMR in guidelines
Role of cardiovascular magnetic resonance in the guidelines of the European Society of Cardiology.

Despite enthusiasm for CMR, its application in Europe is quite diverse. Von Knobelsdorff-Brenkenhoff and Schulz-Menger [51] examined 29 European Society of Cardiology guidelines for their recommendation for CMR and found that only 14/54% of the guidelines contained a specific recommendation regarding CMR. The 14 guidelines had 63 CMR recommendations including 39 class-I recommendations, 12 class II-a recommendations, 10 class-IIb recommendations, and 2 class III recommendations. Nearly 2/3rds of the recommendations were level of evidence C with only 10% level of evidence A. The most common guidelines were for stable coronary artery disease, aortic disease, and hypertrophic cardiomyopathy (HCM).

UK biobank CMR substudy
UK Biobank's cardiovascular magnetic resonance protocol.

The United Kingdom's Biobank's CMR substudy aims to perform CMR studies in 100,000 individuals from the entire 500,000 Biobank cohort of 40-69 year-olds. In this report, Petersen and co-colleagues [52] describe the CMR protocol applied in the UK Biobank's pilot phase which will be extended to three centers. The CMR protocol includes white blood anatomy (sagittal, coronal and transverse), cine (long axis, ventricular short axis, coronal left ventricular outflow tract), strain/tagging, aortic valve flow and parametric native T1.

Normative values - anatomy
Pulmonary artery diameters, cross sectional areas and area changes measured by cine cardiovascular magnetic resonance in healthy volunteers.

Normal diastolic and systolic cross-sectional area of the left main pulmonary artery and its branches are unknown. Burman and co-workers [53] recruited 120 healthy subjects, including 20 (10 males, 10 females) in each decile between 20 and 79 years. Cross sectional areas were rarely circular. Diastolic diameters increased with body surface area (BSA) and age and there was a decrease in distension with age. Normative plots for each decile and gender are provided.

3D black blood VISTA vessel wall cardiovascular magnetic resonance of the thoracic aorta in young, healthy adults: reproducibility and implications for efficacy trial sample sizes: a cross-sectional study.

Preclinical detection of atherosclerosis enables personalized preventive strategies and CMR is an attractive platform for such detection, but data on 3T black blood imaging is lacking. Eikendal and co-workers [54] performed 3T T1 weighted black blood VISTA vessel wall imaging of the aorta in 20 healthy young adults and found excellent inter-scan and inter-rater, and inter-rater data for aortic lumen, total vessel and wall area as well as mean and maximal wall thickness data with sample size estimates required to detect a 5% difference of 203, 126, 136, 68 and 153, respectively.

Cardiovascular magnetic resonance reference ranges for the heart and aorta in Chinese at 3T.

CMR reference ranges have not been well established in Chinese. Le and colleagues [55] performed 3T CMR n 180 healthy Singapore Chinese (20-69 years, 91 men) with image analysis by two observers. Left ventricular (LV) mass was similar in both systole and diastole and stroke volume was similar for the LV and right ventricle (RV). Indexed LV mass was greater in men while indexed atrial sizes and aortic root dimensions were similar. Overall, only 2% of total LV mass was comprised of papillary muscle mass.

Age dependence of pulmonary artery blood flow measured by 4D flow cardiovascular magnetic resonance: results of a population-based study.

Population based pulmonary artery blood flow is unknown. In this prospective study, Wehrum et al. [56] studied 126 age-stratified subjects (at least 20 subjects (10 M/10F) per decade) and found time-to-peak systolic antegrade flow was shorter and peak and average velocities and flow volumes were lower in older subjects. At the end of systole, retrograde flow in the main pulmonary artery was present in all but one subject.

Relationship between body composition and left ventricular geometry using three dimensional cardiovascular magnetic resonance.

Obesity is associated with alterations in left ventricular (LV) mass and volume. In this observational study, Corden and colleagues [57] studied 1530 subjects (mean age 41.3 years; 55% female) without known cardiovascular disease (CVD). LV mass was positively associated with fat mass in women but not in men. Male fat mass was strongly associated with concentric *increase* in relative wall thickness and *reduced* mid-ventricular cavity size.

Between cardiac deformation parameters measured by cardiovascular magnetic resonance and aerobic fitness in endurance athletes.

Athletic training leads to remodeling of both ventricles with increased myocardial mass and biventricular cavity dilation. In this study, Swoboda and co-workers [58] performed CMR tagging in 35 endurance athletes and 35 age and sex matched controls at 3T. LV circumferential strain, twist and torsion, late diastolic longitudinal strain rate and RV peak longitudinal strain, early and late diastolic longitudinal strain rate were all lower in athletes, but on multivariable linear regression, on LV torsion had a significant association with lactate threshold and only RV longitudinal late diastolic strain had a significant association with VO_2 max.

Characterization of left and right atrial function in healthy volunteers by cardiovascular magnetic resonance.

Left and right atrial function changes with advancing age. In this study, Maciera et al. [59] measured maximal, preatrial contraction and minimal left and right atrial volumes in 120 healthy subjects (10 men/10 woman each decile). Gender had an impact on left and right atrial conduit and booster function while age was found to significantly impact most biatrial measures.

Normative values – T1, ECV
Comparison of different cardiovascular magnetic resonance sequences for native myocardial T1 mapping at 3T.

A number of different CMR sequences have been advocated for native T1 mapping.. Comparison data among sequences is sparce at 3T. Teixeira and colleagues [60] compared shortened modified Look-Locker inversion recovery (ShMOLLI), modified Look-Locker inversion recovery (MOLLI) and single-shot acquisition (SASHA) sequences in phantoms and 40 healthy subjects with low or moderate cardiovascular risk at 3T. SASHA provided consistently greater native T1 in subjects and phantoms. On multivariate regression analysis, a longer T1 by MOLLI correlated with a lower left ventricular (LV) ejection fraction and female gender.

Myocardial T1-mapping at 3T using saturation-recovery: reference values, precision and comparison with MOLLI.

Myocardial T1 mapping has become an important quantitative tool for non-invasive tissue characterization for which minimal normative data at 3T are available. Weingartner et al. [61] compared balanced steady-state free precession saturation pulse prepared heart-rate independent inversion recovery (SAPPHIRE) and saturation-recovery single-shot acquisition (SASHA) T1 mapping with Modified Look-Locker Inversion recovery (MOLLI) in 20 healthy subjects (10 men). SAPPHIRE

and SASHA yielded higher T1 time and lower extracellular volume fraction (ECV) compared with MOLLI. All three methods had similar interobserver variation for both T1 and ECV.

Histologic validation of myocardial fibrosis measured by T1 mapping: a systemic review and meta-analysis.

Myocardial fibrosis is being increasingly recognized as a common final pathway for a wide variety of cardiovascular diseases and validation histologic studies of T1 for fibrosis are limited. Diao and colleagues [62] performed a PubMed, EMBASE and Cochrane Library database search for studies applying T1 mapping to measure myocardial fibrosis that validated the results with histological data. A total of 15 studies including 308 patients who had both CMR and biopsy were identified. The pooled correlation between extracellular volume fraction (ECV) and T1 mapping was found to be 0.884 and was not notably heterogeneous.

Prognosis

The prognostic value of CMR [63–66] is being increasingly recognized as adding value to patients with known or suspected cardiovascular disease.

Left ventricular long axis function assessed during cine-cardiovascular magnetic resonance is an independent predictor of adverse cardiac events.

Left ventricular long axis dysfunction is an early marker for many pathologic states. Rangarajan and colleagues [67] studied 400 consecutive patients undergoing CMR and measured mitral annular plane systolic excursion (MAPSE) in the 4-chamber view. During a median follow-up of 14.5 months, patients with a lateral MAPSE <1.11 experienced significantly higher adverse events; a remained a significant predictor after adjustment for established clinical risk factors (age, diabetes, hypertension, NYHA class, LV mass).

Left ventricular long axis strain: a new prognosticator in non-ischemic dilated cardiomyopathy.

Long axis strain represents global longitudinal left ventricular (LV) function. Riffel et al. [68] examined long axis strain in 146 patients with non-ischemic cardiomyopathy and found that long axis strain > – 5% showed a significant higher rate of adverse cardiac events (cardiac death, aborted sudden cardiac death, heart transplantation) independent of late gadolinium enhancement (LGE).

Characterization and clinical significance of right ventricular mechanics in pulmonary hypertension evaluated with cardiovascular magnetic resonance feature tracking.

Prognosis in pulmonary artery hypertension is related to right ventricular (RV) function. In this study, de Siqueira and co-workers [69] retrospectively identified 116 patients with pulmonary artery hypertension who underwent right heart catheterization within a month. Using feature tracking software, they found that RV peak global longitudinal strain was significantly reduced in the group with pulmonary hypertension and normal RV ejection fraction (vs. no pulmonary hypertension and normal RV ejection fraction). After adjustment for 6 clinically meaningful covariates, RV global longitudinal, global longitudinal strain rate, and global circumferential strain rate were independently associated with a composite end-point of all-cause mortality, lung transplantation or worsening NYHA functional class.

Coronary artery disease

CMR myocardial stress testing/perfusion [70–73] assessment as well as the use of CMR to assess myocardial infarction [74–78] continue to be examined in larger, multicenter studies.

Myocardial infarction

Cardiovascular magnetic resonance imaging of myocardial oedema following acute myocardial infarction: is whole heart coverage necessary?

The area-at-risk is useful when assessing the efficacy of reperfusion therapy and novel cardioprotective agents after myocardial infarction. In this study by Hamshere and co-workers [79], CMR was performed in 167 patients after successful primary percutaneous coronary intervention with 82 patients undergoing a novel 3-short axis T2-STIR protocol and 85 both the novel 3-short axis protocol and a conventional 10 slice short-axis late gadolinium enhancement (LGE) protocol. The 3-slice T2-STIR and 10 slice LGE area-at-risk imaging showed a strong correlation with each other and with the angiographic risk scores.

Long-term prognosis of unrecognized myocardial infarction detected with cardiovascular magnetic resonance in an elderly population.

The long-term prognosis of CMR detected unrecognized myocardial infarction is not fully evaluated. Barbier et al. [80] performed late gadolinium enhancement (LGE) CMR in 248 randomly chosen 70 year-olds. During a mean 11 year follow-up, adverse cardiac events occurred in 10% of individuals without infarction scar on CMR, 20% of subjects with unrecognized CMR infarction, and 45% of individuals with known infarction.

Scar quantification by cardiovascular magnetic resonance as an independent predictor of long-term

survival in patients with ischemic heart failure treated by coronary artery bypass graft surgery.

Late gadolinium enhancement (LGE) scar burden is associated with inversely associated with functional recovery after coronary artery bypass graft surgery (CABG). In this study, Kancharla et al. [81] identified 196 patients who had undergone CMR prior to CABG, of whom scar was present in 72%. Over a median follow-up of 8.3 years, there were 64 deaths. There was no significant difference in mortality in the LGE(+) and LGE(−) group (29% vs. 37%, respectively) but in the group with scar, a lower scar burden was independently associated with increased survival.

Antecedent hypertension and myocardial injury in patients with reperfused ST-elevation myocardial infarction.

Antecedent hypertension is associated with poor outcome in patients with ST elevation myocardial infarction (STEMI). Reinstadler et al. [82] studied 792 consecutive STEMI patients reperfused within 12 h of symptom onset. Antecedent hypertension was present in 540 (68%) of patients and was associated with major adverse cardiac events (MACE). There were, however, no significant difference in the area at risk, infarct size, myocardial salvage index, extent of microvascular obstruction, and left ventricular ejection fraction (LVEF) between groups.

Infarct size following complete revascularization in patients presenting with STEMI: a comparison of immediate and staged in-hospital non-infarct related artery PCI subgroups in the CvLPRIT Study.

The CvLPRIT Study showed a trend for improved clinical outcomes in the complete revascularization group in those treated with immediate vs. staged in-hospital approach for multivessel coronary artery disease (CAD) and acute STEMI. Khan and co-workers [83] report on the 93 patients in the CMR substudy of CvLPRIT (63 immediate/30 staged). Patients treated with the staged approach had more visible left ventricular (LV) thrombus and greater incidence of no-reflow. After adjustment for confounders, staged patients had larger infarct size and lower LV ejection fraction (LVEF).

Stress CMR
Perfusion cardiovascular magnetic resonance and fractional flow reserve in patients with angiographic multi-vessel coronary artery disease.

Non-invasive CMR perfusion CMR and invasive fractional flow reserve (FFR) are emerging as the most accurate tools for assessment of myocardial ischemia. In this study, Hussain and co-workers [2] performed 1.5T CMR and FFR in 41 patients with angiographic 2 or 3-vessel coronary artery disease. On a per-patient basis, CMR and FFR detected identical ischemic territories in 19 (46%) patients. On a per-vessel basis, there was concordance in 72% of 123 territories, with CMR identifying fewer or greater ischemic territories in 34% and 12%, respectively.

Quantitative assessment of myocardial blood flow in coronary artery disease by cardiovascular magnetic resonance: comparison of Fermi and distributed parameter modeling against invasive methods.

Absolute quantification of myocardial blood flow (MBF) may improve the diagnosis and prognostication of obstructive coronary artery disease (CAD). In this pilot study, Papanastasiou et al. [84] studied 28 subjects with known or suspected CAD with adenosine stress 3 T CMR. Data were analyzed using the Fermi and distributed parameter modeling. On receiver operator curve (ROC) analysis, the distributed parameter model outperformed the conventional Fermi model on a per vessel and per patient.

Benefits of chronic total coronary occlusion percutaneous intervention in patients with heart failure and reduced ejection fraction: insights from a cardiovascular magnetic resonance study.

Chronic total occlusion percutaneous coronary intervention can improve angina and left ventricular (LV) ejection fraction (LVEF). Cardona and co-workers [85] studied 29 patients with heart failure and reduced ejection fraction and evidence of viability and/or ischemia in a territory supplied by a chronic total occlusion who were successfully treated with a percutaneous coronary intervention. CMR was performed prior to and 6 months after intervention. At 6 months, there was a decrease in LV end-systolic volume and an increase in LVEF. In addition, the number of LV segments demonstrating ongoing perfusion was diminished. Angina and NYHA functional class improved and BNP levels declined.

Technical developments
CMR technical advances continue to dominate the field and the *JCMR* publications. Advances are both in sequence development [86–89], T1 mapping and extracellular volume fraction (ECV) [90–98], T2/T2* mapping [98–104], arrhythmia/motion correction [105–110], 3T [111, 112], flow quantification [113–120], perfusion [121, 122], deformation [123–132], strain [133], diffusion tensor imaging [134] and phantoms [135].

Automated analysis
Improved workflow for quantification of left ventricular volumes and mass using free-breathing motion corrected cine imaging.

Traditional breath-hold cine CMR can be problematic. Free breathing alternatives have relied on multiple averages or real-time imaging. The use of distributed computing was recently proposed as a way to improve clinical workflow with such algorithms. Cross et al. [136] studied 25 patients and 25 healthy subjects with free breathing with averaging and breath-hold balanced steady state free precession (bSSFP) compared with motion corrected re-binning. Motion corrected re-binning and averaged free-breathing compared favorably with bSSFP for left ventricular (LV) mass, end-diastolic volume (EDV) and end-systolic volume (ESV). Both motion corrected re-binning and averaged free-breathing SSFP acquisitions and reconstruction times were shorter than the breath-hold bSSFP method – with an average 37%/ 3 min shorter time for motion corrected re-binning (vs breath-hold SSFP).

Systolic MOLLI T1 mapping with heart-rate dependent pulse sequence sampling scheme is feasible in patients with atrial fibrillation.

The irregular rhythm of atrial fibrillation (AF) may cause inaccurate T1 estimation due to mis-triggering and inadequate magnetization recovery. Zhao et al. [137] used systolic T1 mapping with a heart-rate dependent pulse sequence to overcome this issue. Thirty patients with AF and 13 healthy subjects underwent 3T CMR using a modified Look-Locker Inversion Recovery (MOLLI) sequence. For AF patients, both the fixed and the heart rate dependent sampling scheme were performed in systole and diastole. In healthy subjects, the native T1 and ECV generated from the fixed sampling scheme were lower than the heart-rate dependent and 2nd fixed sampling scheme. In AF patients, more T1 mapping artifacts were found in diastole than in systole. The overall left ventricular (LV) T1 time and ECV were greater with diastolic acquisitions.

Evaluation of an automated method for arterial input function detection for first pass myocardial perfusion cardiovascular magnetic resonance.

Quantitative assessment of myocardial blood flow (MBF) with first-pass perfusion CMR requires a measurement of the arterial input function. In this study, Jacobs et al. [138] propose an automated method to improve the objectivity and reduce processing time. First-pass rest and stress perfusion CMR data were analyzed from 270 clinical studies. Automated imaging processing steps included motion correction, intensity correction, detection of the left ventricle (LV), independent component analysis, and LV pixel thresholding to calculate the arterial input function. Data were compared with manual reference measurements. Their proposed method was successfully processed in 99.63% of the images.

Manual and automated arterial input function were highly correlated and required less processing time that the manual approach with similar myocardial blood flow estimates.

Validation of T2* in-line analysis for tissue iron quantification at 1.5T.

There is a need for a simple on-line T2* analysis for T2* so as to improve analysis reproducibility, especially with low volume centers. In this study, Alam and co-workers [139] compared a clinically validated T2* method and a novel works-in-progress sequence with in-line T2* measurements in 78 iron overload patients and 22 healthy subjects. Liver T2* varied from 0.8 to 35.7 ms and cardiac T2* from 6.0 to 52.3 ms. The novel in-line method had difficulty with accurate delineation of the septum due to artifacts and had some overestimation due to the inability to manually correct for noise by truncation of erroneous later echo times. Reproducibility for the existing method was superior to the in-line method.

The effects of extracellular contrast agent (gadobutrol) on the precision and reproducibility of cardiovascular magnetic resonance feature tracking.

CMR feature tracking is an area receiving considerable interest. In this study, Kuetting and colleagues [140] perform cine mid-ventricular short axis and horizontal long axis cine 1.5T CMR in 40 healthy subjects before and 10-15 min after injection of a double dose of gadobutrol. Feature tracking derived basal, mid and apical peak systolic circumferential strain, peak longitudinal strain, and midventricular epicardial and mid-ventricular peak systolic circumferential strain rate were all *reduced* after gadobutrol . Post-contrast strain assessment also showed higher intra and inter-observer variability.

Accelerated two-dimensional cine DENSE cardiovascular magnetic resonance using compressed sensing and parallel imaging.

Cine displacement encoding and stimulated echoes (DENSE) provides accurate quantitative imaging of cardiac mechanics with rapid displacement and strain analysis, but image acquisition times are relatively long. In this study, Chen et al. [141] describe an accelerated cine DENSE sequence with variable-density spiral k-space sampling and golden angle rotations through time. A compressed sensing method, Block Low-rank Sparsity with Motion-guidance (BLOSM) was also combined with sensitivity encoding (SENSE). For retrospectively-under sampled data, BLOSM-SENSE provided similar or lower root mean square error at rates 2 at rate-2 and lower at rate-4 acceleration compared with SENSE.

Comparison of 3T and 1.5T for T2* magnetic resonance of tissue iron.

T2* CMR tissue iron concentration has improved the outcome of transfusion dependent anemia patients. In this study, Alam and co-workers [142] performed 1.5T and 3T T2* CMR in 104 transfusion dependent patients and 20 healthy subjects. Association between heart and liver T2* at 1.5T and 3T were non-linear and R2* approximately doubled at 3T with linear fits for both heart and liver. Coefficients of variation for intra and inter-observer reproducibility as well as inter-study reproducibility tended to be better at 1.5T. Artifact scores were also significantly worse at 3T black blood.

The impact of hematocrit on oxygenation-sensitive cardiovascular magnetic resonance.

Oxygen sensitive CMR is a promising technique in which images are generated through tissue deoxyhemoglobin which is negatively correlated with signal intensity. In this study, Guensch et al. [143] performed oxygen sensitive CMR in 21 healthy subjects using vasoactive breathing stimuli and repeated after rapid infusion of 1 L of lactated Ringer's solution. Rapid infusion resulted in a fall in hemoglobin while baseline myocardial signal intensity increased, and in males, there was a strong association between the change in hemoglobin concentration and percent change in signal intensity.

Ferumoxytol-enhanced magnetic resonance imaging methodology and normal values at 1.5T and 3T.

Ultrasmall supraparamagnetic particles of iron oxide (USPIO)-enhanced MRI can detect tissue-resident macrophage activity and thereby identify focal cellular inflammation. Stirrat and co-workers [144] studied 20 healthy subjects who underwent late gadolinium enhancement (LGE) imaging at baseline and t2* imaging 24 h after USPIO infusion. Following USPIO, there were changes in R2* at 1.5T in the myocardium, skeletal muscle, kidney, liver, spleen and blood; and at 3T in the myocardium, kidney liver, spleen blood and bone. Tissues showing the greatest ferumoxytol enhancement were the reticuloendothelial system: liver, spleen, and bone marrow.

Robust free-breathing SASHA T1 mapping with high-contrast image registration.

Many widely used myocardial native T1 mapping sequences use breath-hold acquisitions that limit the precision of calculated T1 maps. In this study, Chow et al. [145] propose a novel method for generating high-contrast SAturation-recovery single-SHot Acquisition (SASHA) images to enable a robust image registration approach to free breathing T1 mapping.

Breath-hold SASHA, high-contrast SASHA and MOdified Look-Locker Inversion recovery (MOLLI) images were acquired in 10 subjects. Myocardial T1 from free breathing high-contrast SASHA were similar to breath-hold SASHA. In addition, T1 map quality scores were superior with free breathing high-contrast SASHA.

Compressed sensing real-time cine cardiovascular magnetic resonance: accurate assessment of left ventricular function in a single breath-hold.

Cine CMR accelerated by compressed sensing is used to assess left ventricular (LV) function. Kido and co-workers [146] performed conventional breath-hold cine and breath-hold real-time compressed sensing cine CMR study to obtain a short-axis stack of 8 contiguous images. Total imaging time was shorter with compressed sensing, though compressed sensing had reduced image quality. Conventional and compressed sensing had similar quantitative metrics for all measurements (end-diastolic volume, end-systolic volume, stroke volume, ejection fraction, and mass).

An interactive videogame designed to improve respiratory navigator efficiency in children undergoing cardiovascular magnetic resonance.

Many CMR sequences have long scan durations that necessitate respiratory navigator gating, but breathing patterns are more often inconsistent in children. To address this, Hamlet and colleagues [147] developed a custom software that processed the respiratory navigator image in real-time and provided diaphragmatic position to the patient as a cartoon avatar as visual feedback. Using this approach, average navigator efficiency improved from 33% to 58% and signal-to-noise ratio improved by 5%. There was no difference in either metric between trained and untrained participants.

Flow measurement at the aortic root – impact of location of through-plane phase contrast velocity mapping.

CMR aortic flow is often measured at the sinotubular junction even though placement of the slice just above the aortic valve may be more precise. Bertelsen et al. [148] studied 121 patients >70 years by placing the slice at the sinotubular and valve levels. Overall, stroke volume measured at the sinotubular junction was 13-16% *lower*. Among the 58 patients without any valvulopathy, stroke volume measured at the valve level was closest to that measured by left ventricular stroke volume, but still significantly lower than volumetric values.

A medical device-grade T1 and ECV phantom for global T1 mapping quality assurance – the T1

mapping and ECV Standardization in cardiovascular magnetic resonance (T1MES) program.

T1 mapping and extracellular volume (ECV) have the potential to diagnose disease and monitory therapies, but measurements differ between scanners and pulse sequences. Captur and co-workers [149] designed a phantom incorporating nine clinically relevant ranges of T1 and T2 in blood and myocardium, pre and post-contrast and 1.5 T and 3 T. The coefficient of variation was 1% or less between repeat scans indicating good short-term reproducibility. Reproducible manufacture was established and the device received regulatory clearance from the United States Food and Drug Administration (FDA) and the Conformite Europeene (CE) marketing.

Hemodynamic evaluation in patients with transposition of the great arteries after the arterial switch operation: 4D flow and 2D phase contrast cardiovascular magnetic resonance compared with Doppler echocardiography.

Peak velocity measurements are used to evaluate stenosis in patients with transposition of the great arteries after the arterial switch operation. Jarvis and co-workers [150] performed 4D flow and 2D phase contrast CMR in 19 patients 12-25 years after arterial switch operation for transposition. Data were compared with Doppler echocardiography. Significantly higher peak velocities were found with 4D flow vs 2D phase contrast, with no significant difference between 4D flow and Doppler measurements.

D'Errico L, Lamacie MM, Juan LJ, et al. Effects of slice orientation on reproducibility of sequential assessment of right ventricular volumes and ejection fraction: short-axis vs. transverse SSFP cine cardiovascular magnetic resonance.

Reproducibility of right ventricular (RV) volumes and function are of utmost importance, but the optimal slice orientation for RV measurements is unknown. In this study, D'Errico et al. [151] performed cine CMR in the ventricular short axis and transverse slice orientations in addition to phase velocity mapping of the main pulmonary artery in 18 subjects. Both short axis and transverse imaging slices were found to provide similarly reliable and reproducible measures and thus suitable for baseline and follow-up studies.

Magnetic resonance imaging phantoms for quality-control of myocardial T1 and ECV mapping: specific formulation, long-term stability and variation with heart rate and temperature.

CMR phantoms are needed for quality assurance, but their long-term stability for verification of myocardial T1 and extracellular volume fraction (ECV) are unknown. In this study, Vassilous et al. [152] examined nickel-chloride agarose gel phantoms to mimic blood and myocardial T1, T2, and post-gadolinium T1 and ECV. They found only small relative changes in all the native and post-gadolinium T1 values (up to 9.0%) and ECV (up to 8.3%) over a 12 month period. Native and post-gadolinium T2 had a < 2% change. Temperature sensitivity showed the MOLLI T1 values in the long T1 phantoms increasing by 23.9 ms per degree increase and short T1 phantoms increasing by 0.3 ms per degree increase. There was also a very small increase in ECV with temperature increase.

A clinical combined gadobutrol bolus and slow infusion protocol enabling angiography, inversion recovery whole heart, and late gadolinium enhancement imaging in a single study.

The ability to perform 3D inversion recovery CMR angiography and late gadolinium enhancement (LGE) in the same sequence is desirable. Tandon and co-workers [153] propose the use of a bolus of 0.1 mmol/kg gadobutrol for the time resolved CMR angiogram followed by a slow infusion of 0.02-0.03 ml/s with image navigated 3D inversion recovery balanced steady state free precession initiated 45-60 s after the infusion onset. Data from 10 consecutive pediatric subjects were retrospectively assessed and found to have good image quality.

Improved dark blood imaging of the heart using radial balanced steady state free precession,

Dark blood CMR imaging is typically performed using a breath-hold, dual inversion Cartesian fast spin-echo pulse sequence. In this study, Edelman et al. [154] implemented a novel radial balanced steady state free precession (bSSFP) pulse sequence and examined 6 healthy subjects and 27 patients referred for CMR. In both groups, the single shot dual inversion radial bSSFP images showed fewer motion artifacts with faster acquisition.

Dark blood late gadolinium enhancement.

Bright blood late gadolinium enhancement (LGE) displays excellent contrast between infarcted and normal myocardium, but the contrast between the infarcted myocardium and blood pool is often suboptimal. To address this, Kellman and colleagues [155] developed a black blood LGE sequence in which an inversion recovery T2 preparation pulse was combined with a single shot steady state free precession imaging and respiratory corrected averaging to achieved dark blood LGE images. Thirty patients with subendocardial infarction were studied with the bright blood and dark blood LGE methods. The contrast-to-noise ratio (CNR) of the dark

blood LGE method was 13% lower than the bright blood method, but the CNR between the infarction and blood pool was positive for all of the dark blood cases and was negative for 63% of the bright blood cases.

Feasibility of cardiovascular magnetic resonance derived coronary wave intensity analysis.

Wave intensity analysis of the coronary arteries allows for description of the predominant mechanisms influencing coronary flow during the cardiac cycle. Raphael et al. [156] performed wave intensity analysis by CMR and compared data with invasive Doppler data in 12 arteries (8 left; 4 right). The combination of CMR-derived pressure and velocity data produced the expected pattern of forward and reverse compression and expansion waves with good correlation with invasive data and good intra-study CMR reproducibility.

Diffusion tensor imaging
Relationship between cardiac diffusion tensor imaging parameters and anthropometrics in healthy volunteers.

In-vivo cardiac diffusion tensor imaging (cDTI) is uniquely capable of non-invasively interrogating laminar myocardial dynamics. In this study by Mc-Gill and co-workers [157], 3 T cDTI was performed in 43 subjects during the systolic and diastolic pauses with assessment of global and regional fractional anisotropy, mean diffusivity (MD), helix angle gradient (HAg) and the secondary eigenvector angulation (E2A). All cDTI parameters displayed regional heterogeneity and the heart rate had a significant but clinically small impact on systolic values. Male sex and increasing left ventricular (LV) end-diastolic volume were associated with increased systolic HAg, while diastolic HAg and systolic E2A were both directly related to LV mass and body surface area.

In vivo cardiovascular magnetic resonance of 2D vessel wall diffusion anisotropy in carotid arteries.

Diffusion weighted CMR has shown great potential in discriminating between healthy and diseased vessel tissue by evaluating the apparent diffusion coefficient (ADC). Opriessnig et al. [158] performed high resolution CMR diffusion tensor imaging (DTI) in 12 healthy male subjects at 3 T and found the tangential component as the principle direction of diffusion. Mean vessel wall fractional anisotropy values ranged from 0.7 for the youngest to 0.56 for the oldest subject with a significant linear relationship between fractional anisotropy and age. In addition, a linear trend was seen between radial diffusivity and age.

Vascular imaging

Extension of CMR beyond the heart is increasingly being recognized as important in the complete evaluation of patients with cardiac disease. These include vessel wall/plaque imaging [159, 160] as well as vascular stiffness/compliance [161–167], angiography [168], and limb perfusion [169].

Expansive arterial remodeling of the carotid arteries and its effect on atherosclerotic plaque composition and vulnerability: an in-vivo black-blood 3T CMR study in symptomatic stroke patients.

Expansive remodeling is a feature of vulnerable atherosclerotic plaque. In this study by Saam and co-workers [170], 111 symptomatic patients with acute unilateral ischemic stroke and carotid plaques of at least 2 mm thickness underwent multisequence black-blood 3T CMR of the proximal internal carotid arteries. 78% of the 202 arteries examined showed evidence for atherosclerotic disease with American Heart Association (AHA) lesion type III or higher. They also found significant correlations of the modified remodeling index with lumen area, wall area, vessel area, and wall thickness.

Nonenhanced hybridized arterial spin labeled magnetic resonance angiography of the extracranial carotid arteries using a fast low angle shot readout at 3 Tesla.

Disorders of the extracranial carotid arteries are frequently evaluated by contrast-enhanced CMR angiography, but gadolinium contrast is contraindicated in patients with moderate to severe renal insufficiency due to concerns of nephrogenic systemic fibrosis. In this retrospective report, Kokzoglou and co-workers [171] examine image quality of non-enhanced hybridized arterial spin labeling and contrast enhanced CMR angiography in 37 patients presenting with neurologic symptoms. Contrast enhanced CMR angiography provided the best image quality, while the non-enhanced hybridized arterial spin labeling approach provided image quality that exceeded 2D time-of-flight imaging at the carotid bifurcation and internal and external carotid arteries. Further, all 9 vascular abnormalities of the carotid and intracranial arteries were detected by contrast enhanced CMR angiography and hybrid arterial spin labeling, with no false positives.

Assessment of aortic stiffness by cardiovascular magnetic resonance following the treatment of severe aortic stenosis by TAVI and surgical AVR.

Aortic stiffness is increasingly recognized as an independent predictor of adverse cardiovascular outcomes. In this study, Al Musa and co-workers [172]

performed 1.5 T CMR in 72 patients before and 6 months after surgical aortic valve replacement and transcutaneous aortic valve implantation (TAVI). At 6 months, surgical aortic valve replacement was associated with a significant *decrease* in ascending aortic distensibility/*increased* ascending aortic stiffness and an *increase* in pulse wave velocity. In contrast, no significant change was noted in the (older) TAVI group.

Semi-automatic carotid intraplaque hemorrhage detection and quantification on Magnetization-Prepared Rapid Acquisition Gradient-Echo (MP-RAGE) with optimized threshold selection.

Intraplaque hemorrhage is associated with progression of atherosclerosis and cardiovascular events. Liu and colleagues [173] studied 14 patients scheduled for carotid endarterectomy using MP-RAGE CMR. The presence and area of intraplaque hemorrhage was determined by histology. Optimized intensity thresholds for intraplaque hemorrhage were 1.0× the sternocleidomastoid muscle intensity, 1.6× the adjacent muscle intensity, and 2.2 times the median intensity. Using a semi-automated method with these thresholds, the intraplaque hemorrhage detection sensitivity was 59% and specificity 85%.

Aortic stiffness and its impact on left atrial volumes and function in patients after successful coarctation repair: a multiparametric cardiovascular magnetic resonance study.

As compared with a generally good prognosis for early repair, increased cardiovascular morbidity is present in adults with late aortic coarctation repair. To examine potential causes, Voges et al. [174] performed CMR in 51 patients (median 17 years) 14 +/− 7.5 years after coarctation repair and identified reduced thoracic aortic repair in the entire group. In addition, descending aorta distensibility and pulse wave velocity correlated negatively with age at the time of coarctation repair.

The diagnostic value of non-contrast enhanced quiescent interval single shot (QISS) magnetic resonance angiography at 3T for lower extremity peripheral arterial disease, in comparison to CT angiography.

The high incidence of renal insufficiency in patients with peripheral arterial disease raises the need for non-contrast peripheral arterial options. In this study, Wu and colleagues [175] examined the diagnostic performance of quiescent interval single shot (QISS) CMR angiography at 3 T as compared with computed tomography (CT) angiography in 32 consecutive patients with suspected peripheral arterial disease. QISS CMR angiography was slightly inferior to CT angiography for image quality with similar overall sensitivity and specificity for disease. However, in heavily calcified segments, QISS CMR angiography was superior to CT angiography.

Improved high-resolution pediatric vascular cardiovascular magnetic resonance with gadofosveset-enhanced 3D respiratory navigated, inversion recovery prepared gradient echo readout imaging compared to 3D balanced steady-state free precession readout imaging.

Improved definition of vascular structures is a common indication for CMR in the pediatric population with non-contrast 3D respiratory navigated, T2-prepared fat saturation imaging with a balanced steady state free precession (bSSFP) readout is commonly used. Tandon et al. [176] propose an alternative 3D gradient echo inversion recovery sequence with a blood pool agent, gadofosveset trisodium and examined 35 patients with both sequences. The contrast-enhanced 3D inversion recovery sequence had superior overall image quality (including patients with intrathoracic metal) for the right coronary artery, pulmonary arteries/veins and blood pool homogeneity. Signal-to-noise (SNR) and contrast-to-noise (CNR) were also superior for the left atrium and left ventricle, but not the pulmonary arteries.

Co-existing intracranial and extracranial carotid artery atherosclerosis plaques and recurrent stroke risk: a three-dimensional multicontrast cardiovascular magnetic resonance study.

As a systemic disease, atherosclerosis commonly affects intracranial and extracranial carotid arteries simultaneously. In this study, Xu and colleagues [177] examined 58 patients with recent anterior circulation cerebrovascular symptoms and at least one carotid plaque for multiparametric CMR. Co-existing intracranial and extracranial plaque was found in 78%. For those with stroke, the presence of both intracranial and extracranial plaque was associated with recurrent stroke, even after adjusting for traditional clinical risk factors.

Animal models

Small and large animal models continue to play an important role in advancing our understanding of cardiovascular disease [178–185].

Myocardial T1 maps reflect histological findings in acute and chronic stages of myocarditis in a rat model.

CMR offers both diagnostic and prognostic information for myocarditis. In this rat model study, Jeuthe and co-workers [186] immunized male young Lewis rats with porcine myocardial myosin and performed native and contrast-enhanced CMR prior to and on days 14, 21,

and 35. All immunized rats developed myocarditis with histologic wall thickening and biventricular macrophage-rich mixed inflammatory infiltrates. CMR demonstrated increased native myocardial T1 and decreased post-contrast T1.

A new automatic algorithm for quantification of myocardial infarction imaged by late gadolinium enhancement cardiovascular magnetic resonance: experimental validation and comparison to expert delineations in multi-center, multi-vendor patient data.

Late gadolinium enhancement (LGE) CMR using inversion recovery or phase sensitive inversion recovery (PSIR) has become one of the most widely employed CMR clinical sequences in the assessment of patients with known or suspected coronary artery disease. However, there is no clinical standard for infarction quantification. In this study, Engblom and colleagues [187] apply a novel automated algorithm on data derived from 7 swine and with 124 patients from a multi-center, multi-vendor ST elevation study. Infarct size by the automated algorithm in swine showed a slight bias to ex-vivo triphenyltetrazolium chloride (TTC) staining while the patient study showed the automated algorithm showed a slight bias to expert delineation.

Cardiovascular magnetic resonance detectgs the progression of impaired myocardial perfusion reserve and increased left-ventricular mass in mice fed a high-fat diet.

Impaired myocardial perfusion reserve (MPR) is prevalent in obesity and diabetes even in the absence of obstructive coronary artery disease. Naresh and co-workers [188] studied C57Bl/6 mice fed a high-fat or low-fat diet and imaging at 6, 12, 18, and 24 weeks post-diet. Body weight, left ventricular (LV) mass and wall thickness were increased and MPR reduced in the high-fat cohort at 18 and 24 weeks. Coronary artery vascular reactivity to adenosine and acetylcholine was also reduced in the high-fat cohort.

Early-stage heart failure with preserved ejection fraction in the pig: a cardiovascular magnetic resonance study.

A hypertensive deoxy-corticosterone acetate salt-treated pig model of early stage heart failure with preserved ejection fraction (HFpEF). Reiter and colleagues [189] studied 5 HFpEF swine and 6 controls with dobutamine stress at 3 T. They found the HFpEF swine had increased left ventricular (LV) mass and wall thickness along with increase left atrial volume. Myocardial perfusion reserve was decreased

in the HFpEF swine. T1 time did not differ between groups.

Congenital heart disease

The non-ionizing multiparametric attributes of CMR make it ideal for imaging of the pediatric and adult patient with known or suspected congenital heart disease [190–194] including blood flow [195]).

Tetralogy of Fallot

Vicious circle between progressive right ventricular dilation and pulmonary regurgitation in patients after tetralogy of Fallow Repair. Right heart enlargement promotes flow reversal in the left pulmonary artery.

The left pulmonary artery contributes more than the right pulmonary artery to total pulmonary regurgitation in patients after tetralogy of Fallot (TOF) repair. Kato and co-workers [196] studied 48 patients with TOF repair and found no difference in left and right pulmonary artery diameters, but the left pulmonary artery had less total forward flow, smaller net forward flow, and greater regurgitant fraction. There was no difference in regurgitant flow volume. Indexed right ventricular end-diastolic volume correlate4d with left pulmonary artery regurgitant fraction, but not with right pulmonary artery regurgitant fraction.

Left and right ventricular dyssynchrony and strains from cardiovascular magnetic resonance feature tracking do not predict deterioration of ventricular function in patients with repaired tetralogy of Fallot.

Patients with repaired tetralogy of Fallot (TOF) suffer from progressive ventricular dysfunction decades after surgical repair. In this study, Jing et al. [197] retrospectively identified 153 repaired TOF patients who had at least 2 CMRs performed >6 month apart without intervening mechanical intervention. After a mean follow-up of 2.9 years, no feature tracking metric (interventricular dyssnchrony, left ventricular (LV) and right ventricular (RV) peak global circumferential strain and LV and RV peak global longitudinal strain) was associated with adverse outcomes or ventricular remodeling.

Increased left ventricular myocardial extracellular volume is associated with longer cardiopulmonary bypass times, biventricular enlargement and reduced exercise tolerance in children after repair of Tetralogy of Fallot.

Unfavorable left ventricular (LV) remodeling may be associated with adverse remodeling after repair of tetralogy of Fallot (TOF). In this cross-sectional, prospective study, Riesenkampff and co-workers [198] studied 31 TOF repair subjects and 15 controls and found no

difference in native T1 or extracellular volume fraction (ECV) between TOF and controls, though the female TOF cohort had a higher ECV than male TOF cohort. In the TOF group, higher native T1 and ECV correlated with higher Z-scores of right ventricular (RV) and LV end-diastolic value but not with reduced LV or RV ejection fraction. Higher native T1 did correlate with worse LV longitudinal and mid short axis circumferential strain.

Miscellaneous topics/reviews

CMR assessment of blood flow [199] and image processing [200] are likely to play an increasing role in the assessment of our patients and automated analyses of the growing image datasets. Helping clinicians understand the role of CMR amongst all of the cardiovascular imaging will also be of increasing importance.

Physician's professional identities: a roadmap to understanding "value" in cardiovascular imaging.

Quality improvement efforts have been challenged by limited adoption of initiatives and policies. In this study, Keller and co-workers [201] interviewed 15 Northwestern Medicine physicians from internal medicine, cardiology, emergency medicine, cardiac/vascular surgery, and radiology disciplines. Differences in perceived cardiovascular imaging value and guideline use were explained by three value associated categories (managers; diagnosticians; and fixers) that were further differentiated along three axes (broad v. focused-thinkers; complex v. definitive-answer seekers; and public visibility).

Use of self-gated radial cardiovascular magnetic resonance to detect and classify arrhythmias (atrial fibrillation and premature ventricular contraction).

Arrhythmias can degrade CMR image quality. As a result, automated detection and sorting of the most frequent types of arrhythmias may improve image quality. Piekarski and colleagues [202] retrospectively studied 111 patients who underwent self-gated free-breathing radial cardiac cine CMR with compressed sensing reconstruction for detection of atrial fibrillation, premature ventricular contractions, and non-sinus rhythm to detect non-sinus rhythm. Using their algorithm to identify non-sinus rhythm, sensitivity, specificity and accuracy was 93%, 95% and 94% respectively to discriminate non-arrhythmic and arrhythmic patients and 83%, 71% and 77% to discriminate atrial fibrillation and premature ventricular contractions.

Top 100 cited articles in cardiovascular magnetic resonance: a bibliometric analysis.

Bibliometric studies can help guide researchers and research funding agencies toward areas where allocation or increase in research activity is warranted. Khan and co-workers [203] performed a Web of Science search to identify all CMR publications to identify the top 100 cited articles. The vast majority (86%) of manuscripts were published between 2000 and 2014 and 17 articles were cited more than 500 times. A total of 52% were from the United States and 21% from the United Kingdom. *Circulation* and *the Journal of the American College of Cardiology* published 62% of the articles.

Myocardial triglyceride content at 3T cardiovascular magnetic resonance and left ventricular systolic function: a cross-sectional study in patients hospitalized with acute heart failure.

Increased myocardial triglyceride (TG) content has been recognized as a risk factor for cardiovascular disease. Liao et al. [204] performed 3 T CMR 1H spectroscopy in 50 patients (including 25 with left ventricular ejection fraction <50%) discharged after hospitalization for acute heart failure and 21 age and sex matched controls. Myocardial unsaturated fatty acid/water ratio was found to be differ (0.79% vs. 0.21% vs. 0.14%) between the low ejection fraction heart failure, normal ejection fraction heart failure and healthy controls, respectively.

Reviews

Focused reviews are an important component of the *JCMR* educational process, especially with the rapid advances made in the CMR field. In 2016, reviews were published on myocardial spin labeling [205], extracardiac findings seen on CMR [206], feature tracking [207], Takotsubo cardiomyopathy [208], T1 and ECV [209].

Case report

Detection of metallic cobalt and chromium liver deposition followed failed hip replacement using T2* and R2 magnetic resonance.

In 2016, the *JCMR* had a single case report of a patient with cobalt and chromium liver deposition following a failed hip replacement [210]. It is not anticipated that there will be any case reports in 2017 and beyond. Those interested in publishing a CMR case report are encouraged to submit their work to the case series on the SCMR web site (www.scmr.org).

cardiac event; MAPSE: Mitral annular plane systolic excursion; MBF: Myocardial blood flow; MOLLI: Modified Look-Locker inversion recovery; MPR: Myocardial perfusion reserve; NYHA: New York Heart Association; QISS: Quiescent interval single shot; RV: Right ventricle/right ventricular; SASHA: Single shot acquisition; SCMR: Society for Cardiovascular Magnetic Resonance; SENSE: Sensitivity encoding; ShMOLLI: Shortened modified Look-Locker inversion recover; SNR: Signal-to-noise ratio; STEMI: ST elevation myocardial infarction; TAVI: Transcutaneous aortic valve implantation; TOF: Tetralogy of Fallot; USPIO: Ultrasmall particles of iron oxide

References
1. Chan AT, Plodkowski AJ, Pun SC, et al. Prognostic utility of differential tissue characterization of cardiac neoplasm and thrombus via late gadolinium enhancement cardiovascular magnetic resonance among patients with advanced systemic cancer. J Cardiovasc Magn Reson. 2017;19:76.
2. Hussain ST, Chiribiri A, Morton G, et al. Perfusion cardiovascular magnetic resonance and fractional flow reserve in patients with angiographic multi-vessel coronary artery disease. J Cardiovasc Magn Reson. 2016;18:44.
3. Pennell DJ, Baksi AJ, Prasad SK, Raphael CE, Kilner PJ, Mohiaddin RH, Alpendurada F, Babu-Narayan SV, Schneider J, Firmin DN. Review of journal of cardiovascular magnetic resonance 2014. J Cardiovasc Magn Reson. 2015;17:99.
4. Reant P, Captur G, Mirabel M, Nasis A, Sado DA, Maestrini V, Castelletti S, Manisty C, Herrey AS, Syrris P, Tome-Esteban M, Jenkins S, Elliott PM, McKenna WJ, Moon JC. Abnormal septal convexity into the left ventricle occurs in subclinical hypertrophic cardiomyopathy. J Cardiovasc Magn Reson. 2015;17:64.
5. Nguyen C, Lu M, Fan Z, Bi X, Kellman P, Zhao S, Li D. Contrast-free detection of myocardial fibrosis in hypertrophic cardiomyopathy patients with diffusion-weighted cardiovascular magnetic resonance. J Cardiovasc Magn Reson. 2015;17:107.
6. Kozor R, Callaghan F, Tchan M, Hamilton-Craig C, Figtree GA, Grieve SM. A disproportionate contribution of papillary muscles and trabeculations to total left ventricular mass makes choice of cardiovascular magnetic resonance analysis technique critical in Fabry disease. J Cardiovasc Magn Reson. 2015;17:22.
7. Ng MY, Li Q, Calleja A, Deva DP, Crean AM, Gruner C, Iwanochko RM, Thavendiranathan P. Erratum: relationship between MRI derived right ventricular mass and left ventricular involvement in patients with Anderson-Fabry disease. J Cardiovasc Magn Reson. 2015;17:42.
8. Latus H, Gummel K, Klingel K, Moysich A, Khalil M, Mazhari N, Bauer J, Kandolf R, Schranz D, Apitz C. Focal myocardial fibrosis assessed by late gadolinium enhancement cardiovascular magnetic resonance in children and adolescents with dilated cardiomyopathy. J Cardiovasc Magn Reson. 2015;17:34.
9. Florian A, Ludwig A, Stubbe-Dräger B, Boentert M, Young P, Waltenberger J, Rösch S, Sechtem U, Yilmaz A. Characteristic cardiac phenotypes are detected by cardiovascular magnetic resonance in patients with different clinical phenotypes and genotypes of mitochondrial myopathy. J Cardiovasc Magn Reson. 2015;17:40.
10. Pöyhönen P, Hiippala A, Ollila L, Kaasalainen T, Hänninen H, Heliö T, Tallila J, Vasilescu C, Kivistö S, Ojala T, Holmström M. Cardiovascular magnetic resonance findings in patients with PRKAG2 gene mutations. J Cardiovasc Magn Reson. 2015;17:89.
11. Diaz-Zamudio M, Dey D, LaBounty T, Nelson M, Fan Z, Szczepaniak LS, Hsieh BP, Rajani R, Berman D, Li D, Dharmakumar R, Hardy WD, Conte AH. Increased pericardial fat accumulation is associated with increased

intramyocardial lipid content and duration of highly active antiretroviral therapy exposure in patients infected with human immunodeficiency virus: a 3T cardiovascular magnetic resonance feasibility study. J Cardiovasc Magn Reson. 2015;17:91.
12. Cheng H, Lu M, Hou C, Chen X, Li L, Wang J, Yin G, Chen X, Xiangli W, Cui C, Chu J, Zhang S, Prasad SK, Pu J, Zhao S. Comparison of cardiovascular magnetic resonance characteristics and clinical consequences in children and adolescents with isolated left ventricular non-compaction with and without late gadolinium enhancement. J Cardiovasc Magn Reson. 2015;17:44.
13. Sanguineti F, Garot P, Mana M, O'h-Ici D, Hovasse T, Unterseeh T, Louvard Y, Troussier X, Morice MC, Garot J. Cardiovascular magnetic resonance predictors of clinical outcome in patients with suspected acute myocarditis. J Cardiovasc Magn Reson. 2015;17:78.
14. Banka P, Robinson JD, Uppu SC, Harris MA, Hasbani K, Lai WW, Richmond ME, Fratz S, Jain S, Johnson TR, Maskatia SA, Lu JC, Samyn MM, Patton D, Powell AJ. Cardiovascular magnetic resonance techniques and findings in children with myocarditis: a multicenter retrospective study. J Cardiovasc Magn Reson. 2015;17:96.
15. Jeserich M, Merkely B, Olschewski M, Kimmel S, Pavlik G, Bode C. Patients with exercise-associated ventricular ectopy present evidence of myocarditis. J Cardiovasc Magn Reson. 2015;17:100.
16. Bietenbeck M, Florian A, Sechtem U, Yilmaz A. The diagnostic value of iron oxide nanoparticles for imaging of myocardial inflammation - quo vadis? J Cardiovasc Magn Reson. 2015;17:54.
17. Torreão JA, Ianni BM, Mady C, Naia E, Rassi CH, Nomura C, Parga JR, Avila LF, Ramires JA, Kalil-Filho R, Rochitte CE. Myocardial tissue characterization in Chagas' heart disease by cardiovascular magnetic resonance. J Cardiovasc Magn Reson. 2015;17:97.
18. Alam MH, Auger D, Smith GC, He T, Vassiliou V, Baksi AJ, Wage R, Drivas P, Feng Y, Firmin DN, Pennell DJ. T1 at 1.5T and 3T compared with conventional T2* at 1.5T for cardiac siderosis. J Cardiovasc Magn Reson. 2015;17:102.
19. Mehta BB, Auger DA, Gonzalez JA, Workman V, Chen X, Chow K, Stump CJ, Mazimba S, Kennedy JL, Gay E, Salerno M, Kramer CM, Epstein FH, Bilchick KC. Detection of elevated right ventricular extracellular volume in pulmonary hypertension using accelerated and navigator-gated look-locker imaging for cardiac T1 estimation (ANGIE) cardiovascular magnetic resonance. J Cardiovasc Magn Reson. 2015;17:110.
20. Knight DS, Steeden JA, Moledina S, Jones A, Coghlan JG, Muthurangu V. Left ventricular diastolic dysfunction in pulmonary hypertension predicts functional capacity and clinical worsening: a tissue phase mapping study. J Cardiovasc Magn Reson. 2015;17:116.
21. Villa ADM, Sammut E, Zarinabad N, et al. Microvascular ischemia in hypertrophic cardiomyopathy: new insights from high-resolution combined quantification of perfusion and late gadolinium enhancement. J Cardiovasc Magn Reson. 2016;18:4.
22. Tarkiainen M, Sipola P, Jalanko M, et al. Cardiovascular magnetic resonance of mitral valve length in hypertrophic cardiomyopathy. J Cardiovasc Magn Reson. 2016;18:33.
23. Deva DP, Hanneman K, Li Q, et al. Cardiovascular magnetic resonance demonstration of the spectrum of morphological phenotypes and patterns of myocardial scarring in Anderson-Fabry disease. J Cardiovasc Magn Reson. 2016;18:14.
24. Li R, Yang Z, Wen L, et al. Regional myocardial microvascular dysfunction in cardiac amyloid light-chain amyloidosis: assessment with 3T cardiovascular magnetic resonance. J Cardiovasc Magn Reson. 2016;18:16.
25. Taylor RJ, Umarn F, Lin ELS, et al. Mechanical effects of left ventricular midwall fibrosis in non-ischemic cardiomyopathy. J Cardiovasc Magn Reson. 2016;18:1.
26. Chitiboi T, Schnell S, Collins J, et al. Analyzing myocardial torsion based on tissue phase mapping cardiovascular magnetic resonance. J Cardiovasc Magn Reson. 2016;18:15.
27. Kato S, Nakamori S, Roujol S, et al. Relationship between native papillary muscle T1 time and severity of functional mitral regurgitation in patients with non-ischemic dilated cardiomyopathy. J Cardiovasc Magn Reson. 2016;18:79.
28. Mikami Y, Cornhill A, Heydari B, et al. Objective criteria for septal fibrosis in non-ischemic dilated cardiomyopathy: validation for the prediction of future cardiovascular events. J Cardiovasc Magn Reson. 2016;18:82.
29. Soslow JH, Damon SM, Crum K, et al. Increased myocardial native T1 and extracellular volume in patients with Duchenne muscular dystrophy. J Cardiovasc Magn Reson. 2016;18:5.
30. Becker S, Florian A, Patrascu A, et al. Identification of cardiomyopathy associated circulating miRNA biomarkers in patients with muscular

dystrophy using a complementary cardiovascular magnetic resonance and plasma profiling approach. J Cardiovasc Magn Reson. 2016;18:25.

31. Wexberg P, Avanzini M, Mascherbauer J, et al. Myocardial late gadolinium enhancement is associated with clinical presentation in Duchenne muscular dystrophy. J Cardiovasc Magn Reson. 2016;18:61.

32. Olivieri LJ, Kellman P, McCarter RJ, et al. Native T1 values identify myocardial changes and disease severity in patients with Duchenne muscular dystrophy. J Cardiovasc Magn Reson. 2016;18:72.

33. Choi Y, Kim SM, Lee SC, et al. Quantification of left ventricular trabeculae using cardiovascular magnetic resonance for the diagnosis of left ventricular non-compaction: evaluation of trabecular volume and refined semi-quantitative criteria. J Cardiovasc Magn Reson. 2016;18:24.

34. Assuncao AN, Jerosch-Herold M, Melo RL, et al. Chagas' heart disease: gender differences in myocardial damage assessed by cardiovascular magnetic resonance. J Cardiovasc Magn Reson. 2016;18:88.

35. Boentert M, Florian A, Drager B, et al. Pattern and prognostic value of cardiac involvement in patients with late-onset Pompe disease: a comprehensive cardiovascular magnetic resonance approach. J Cardiovasc Magn Reson. 2016;18:91.

36. Jing L, Binklehy CM, Suever JD. Cardiac remodeling and dysfunction in childhood obesity: a cardiovascular magnetic resonance study. J Cardiovasc Magn Reson. 2016;18:28.

37. Mayr A, Kitterer D, Latus J, et al. Evaluation of myocardial involvement in patients with connective tissue disorders: a multi-parametric cardiovascular magnetic resonance study. J Cardiovasc Magn Reson. 2016;18:67.

38. Krumm P, Mueller KAL, Klingel K, et al. Cardiovascular magnetic resonance patterns of biopsy proven cardiac involvement in systemic sclerosis. J Cardiovasc Magn Reson. 2016;18:70.

39. McLeod K, Wall S, Leren IS, et al. Ventricular structure in ARVC: going beyond volumes as a measure of risk. J Cardiovasc Magn Reson. 2016;18:73.

40. Mygind ND, Michelsen MM, Pena A, et al. Coronary microvascular function and myocardial fibrosis in women with angina pectoris and no obstructive coronary artery disease: the iPOWER study. J Cardiovasc Magn Reson. 2016;18:76.

41. Bruder O, Schneider S, Pilz G, van Rossum AC, Schwitter J, Nothnagel D, Lombardi M, Buss S, Wagner A, Petersen S, Greulich S, Jensen C, Nagel E, Sechtem U, Mahrholdt H. 2015 Update on acute adverse reactions to gadolinium based contrast agents in cardiovascular MR. large multinational and multi-ethnical population experience with 37788 patients from the EuroCMR registry. J Cardiovasc Magn Reson. 2015;17:58.

42. McGraw S, Mirza O, Bauml MA, Rangarajan VS, Farzaneh-Far A. Downstream clinical consequences of stress cardiovascular magnetic resonance based on appropriate use criteria. J Cardiovasc Magn Reson. 2015;17:35.

43. Klein-Wiele O, Garmer M, Urbien R, Busch M, Kara K, Mateiescu S, Grönemeyer D, Schulte-Hermes M, Garbrecht M, Hailer B. Feasibility and safety of adenosine cardiovascular magnetic resonance in patients with MR conditional pacemaker systems at 1.5 Tesla. J Cardiovasc Magn Reson. 2015;17:112.

44. Yi CJ, Wu CO, Tee M, Liu CY, Volpe GJ, Prince MR, Hundley GW, Gomes AS, van der Geest RJ, Heckbert S, Lima JA, Bluemke DA. The association between cardiovascular risk and cardiovascular magnetic resonance measures of fibrosis: the multi-ethnic study of atherosclerosis (MESA). Cardiovasc Magn Reson. 2015;17:15.

45. Kawel-Boehm N, Maceira A, Valsangiacomo-Buechel ER, Vogel-Claussen J, Turkbey EB, Williams R, Plein S, Tee M, Eng J, Bluemke DA. Normal values for cardiovascular magnetic resonance in adults and children. J Cardiovasc Magn Reson. 2015;17:29.

46. Suinesiaputra A, Bluemke DA, Cowan BR, Friedrich MG, Kramer CM, Kwong R, Plein S, Schulz-Menger J, Westenberg JJM, Young AA, Nagel E. Quantification of LV function and mass by cardiovascular magnetic resonance: multi-center variability and consensus contours. J Cardiovasc Magn Reson. 2015;17:63.

47. Kowallick JT, Morton G, Lamata P, Jogiya R, Kutty S, Hasenfuß G, Lotz J, Nagel E, Chiribiri A, Schuster A. Quantification of atrial dynamics using cardiovascular magnetic resonance: inter-study reproducibility. J Cardiovasc Magn Reson. 2015;17:36.

48. Zareian M, Ciuffo L, Habibi M, Opdahl A, Chamera EH, Wu CO, Bluemke DA, Lima JAC, Venkatesh BA. Left atrial structure and functional quantitation using cardiovascular magnetic resonance and multimodality tissue tracking: validation and reproducibility assessment. J Cardiovasc Magn Reson. 2015;17:52.

49. Karakus G, Kammerlander AA, Aschauer S, Marzluf BA, Zotter-Tufaro C, Bachmann A, Degirmencioglu A, Duca F, Babayev J, Pfaffenberger S, Bonderman D, Mascherbauer J. Pulmonary artery to aorta ratio for the detection of pulmonary hypertension: cardiovascular magnetic resonance and invasive hemodynamics in heart failure with preserved ejection fraction. J Cardiovasc Magn Reson. 2015;17:79.

50. Moschetti K, Petersen SE, Pilz G, et al. Cost-minimization analysis of three decision strategies for cardiac revascularization: results of the "suspected CAD" cohort of the European cardiovascular magnetic resonance registry. J Cardiovasc Magn Reson. 2016;18:3.

51. von Knobelsdorff-Brenkenhoff F, Schulz-Menger J. Role of cardiovascular magnetic resonance in the guidelines of the European Society of Cardiology. J Cardiovasc Magn Reson. 2016;18:6.

52. Petersen SE, Matthews PM, Francis JM, et al. UK Biobank's cardiovascular magnetic resonance protocol. J Cardiovasc Magn Reson. 2016;18:8.

53. Burman ED, Keegan HJ, Kilner PJ. Pulmonary artery diameters, cross sectional areas and area changes measured by cine cardiovascular magnetic resonance in healthy volunteers. J Cardiovasc Magn Reson. 2016;18:12.

54. Eikendal ALM, Blomberg BA, Haaring C, et al. 3D black blood VISTA vessel wall cardiovascular magnetic resonance of the thoracic aorta in young, healthy adults: reproducibility and implications for efficacy trial sample sizes: a cross-sectional study. J Cardiovasc Magn Reson. 2016;18:20.

55. Le TT, Tan RS, Deyn AD, et al. Cardiovascular magnetic resonance reference ranges for the heart and aorta in Chinese at 3T. J Cardiovasc Magn Reson. 2016;18:21.

56. Wehrum T, Hagenlocher P, Lodrmann T, et al. Age dependence of pulmonary artery blood flow measured by 4D flow cardiovascular magnetic resonance: results of a population-based study. J Cardiovasc Magn Reson. 2016;18:31.

57. Corden B, de Marvao A, Dawes TJ, et al. Relationship between body composition and left ventricular geometry using three dimensional cardiovascular magnetic resonance. J Cardiovasc Magn Reson. 2016;18:32.

58. Swoboda PP, Erhayiem B, McDiarmid AK, et al. Relationship between cardiac deformation parameters measured by cardiovascular magnetic resonance and aerobic fitness in endurance athletes. J Cardiovasc Magn Reson. 2016;18:48.

59. Maciera AM, Cosin-Sales J, Prasad SK, et al. Characterization of left and right atrial function in healthy volunteers by cardiovascular magnetic resonance. J Cardiovasc Magn Reson. 2016;18:64.

60. Teixeira T, Hafyane T, Stikov N, et al. Comparison of different cardiovascular magnetic resonance sequences for native myocardial T1 mapping at 3T. J Cardiovasc Magn Reson. 2016;18:65.

61. Weingartner S, Messner NM, Budjan J, et al. Myocardial T1-mapping at 3T using saturation-recovery: reference values, precision and comparison with MOLLI. J Cardiovasc Magn Reson. 2016;18:84.

62. Diao K, Yang Z, Xu H, et al. Histologic validation of myocardial fibrosis measured by T1 mapping: a systemic review and meta-analysis. J Cardiovasc Magn Reson. 2016;18:92.

63. Sukpraphrute B, Drafts BC, Rerkpattanapipat P, Morgan TM, Kirkman PM, Ntim WO, Hamilton CA, Cockrum RL, Hundley WG. Prognostic utility of cardiovascular magnetic resonance upright maximal treadmill exercise testing. J Cardiovasc Magn Reson. 2015;17:103.

64. Hauser TH, Essebag V, Baldessin F, McClennen S, Yeon SB, Manning WJ, Josephson ME. Prognostic value of pulmonary vein size in prediction of atrial fibrillation recurrence after pulmonary vein isolation: a cardiovascular magnetic resonance study. J Cardiovasc Magn Reson. 2015;17:49.

65. Hartlage GR, Suever JD, Clement-Guinaudeau S, Strickland PT, Ghasemzadeh N, Magrath RP, Parikh A, Lerakis S, Hoskins MH, Leon AR, Lloyd MS, Oshinski JN. Prediction of response to cardiac resynchronization therapy using left ventricular pacing lead position and cardiovascular magnetic resonance derived wall motion patterns: a prospective cohort study. J Cardiovasc Magn Reson. 2015;17:57.

66. Kato S, Sekine A, Kusakawa Y, Ogura T, Futaki M, Iwasawa T, Kirigaya H, Gyotoku D, Iinuma N, Iguchi K, Nakachi T, Fukui K, Kimura K, Umemura S. Prognostic value of cardiovascular magnetic resonance derived right ventricular function in patients with interstitial lung disease. J Cardiovasc Magn Reson. 2015;17:10.

67. Rangarajan V, Chacko SJ, Romano S, et al. Left ventricular long axis function assessed during cine-cardiovascular magnetic resonance is an independent predictor of adverse cardiac events. J Cardiovasc Magn Reson. 2016;18:35.

68. Riffel JH, Keller MGP, Rost F, et al. Left ventricular long axis strain: a new prognosticator in non-ischemic dilated cardiomyopathy. J Cardiovasc Magn Reson. 2016;18:36.

69. De Siqueira MEM, Pozo E, Fernandes VR, et al. Characterization and clinical significance of right ventricular mechanics in pulmonary hypertension evaluated with cardiovascular magnetic resonance feature tracking. J Cardiovasc Magn Reson. 2016;18:39.

70. Ripley DP, Motwani M, Brown JM, Nixon J, Everett CC, Bijsterveld P, Maredia N, Plein S, Greenwood JP. Individual component analysis of the multi-parametric cardiovascular magnetic resonance protocol in the CE-MARC trial. J Cardiovasc Magn Reson. 2015;17:59.

71. Greulich S, Steubing H, Birkmeier S, Grün S, Bentz K, Sechtem U, Mahrholdt H. Impact of arrhythmia on diagnostic performance of adenosine stress CMR in patients with suspected or known coronary artery disease. J Cardiovasc Magn Reson. 2015;17:94.

72. Vasu S, Little WC, Morgan TM, Stacey RB, Ntim WO, Hamilton C, Thohan V, Chiles C, Hundley WG. Mechanism of decreased sensitivity of dobutamine associated left ventricular wall motion analyses for appreciating inducible ischemia in older adults. J Cardiovasc Magn Reson. 2015;17:26.

73. Sampaio F, Lamata P, Bettencourt N, Alt SC, Ferreira N, Kowallick JT, Pimenta J, Kutty S, Fraga J, Steinmetz M, Bettencourt P, Gama V, Schuster A. Assessment of cardiovascular physiology using dobutamine stress cardiovascular magnetic resonance reveals impaired contractile reserve in patients with cirrhotic cardiomyopathy. J Cardiovasc Magn Reson. 2015;17:61.

74. Rodríguez-Palomares JF, Ortiz-Pérez JT, Lee DC, Bucciarelli-Ducci C, Tejedor P, Bonow RO, Wu E. Time elapsed after contrast injection is crucial to determine infarct transmurality and myocardial functional recovery after an acute myocardial infarction. J Cardiovasc Magn Reson. 2015;17:43.

75. Eitel I, Pöss J, Jobs A, Eitel C, de Waha S, Barkhausen J, Desch S, Thiele H. Left ventricular global function index assessed by cardiovascular magnetic resonance for the prediction of cardiovascular events in ST-elevation myocardial infarction. J Cardiovasc Magn Reson. 2015;17:62.

76. Bulluck H, White SK, Rosmini S, Bhuva A, Treibel TA, Fontana M, Abdel-Gadir A, Herrey A, Manisty C, Wan SM, Groves A, Menezes L, Moon JC, Hausenloy DJ. T1 mapping and T2 mapping at 3T for quantifying the area-at-risk in reperfused STEMI patients. J Cardiovasc Magn Reson. 2015;17:73.

77. Hammar P, Nordenskjöld AM, Lindahl B, Duvernoy O, Ahlström H, Johansson L, Hadziosmanovic N, Bjerner T. Unrecognized myocardial infarctions assessed by cardiovascular magnetic resonance are associated with the severity of the stenosis in the supplying coronary artery. J Cardiovasc Magn Reson. 2015;17:98.

78. Oduneye SO, Pop M, Shurrab M, Biswas L, Ramanan V, Barry J, Crystal E, Wright GA. Distribution of abnormal potentials in chronic myocardial infarction using a real time magnetic resonance guided electrophysiology system. J Cardiovasc Magn Reson. 2015;17:27.

79. Hamshere S, Jones DA, Pellaton C, et al. Cardiovascular magnetic resonance imaging of myocardial oedema following acute myocardial infarction: is whole heart coverage necessary? J Cardiovasc Magn Reson. 2016;18:7.

80. Barbier CE, Themudo R, Bjerner T, et al. Long-term prognosis of unrecognized myocardial infarction detected with cardiovascular magnetic resonance in an elderly population. J Cardiovasc Magn Reson. 2016;18:43.

81. Kancharla K, Weissman G, Elagha AA, et al. Scar quantification by cardiovascular magnetic resonance as an independent predictor of long-term survival in patients with ischemic heart failure treated by coronary artery bypass graft surgery. J Cardiovasc Magn Reson. 2016;18:45.

82. Reinstadler SJ, Stiermaier T, Eitel C, et al. Antecedent hypertension and myocardial injury in patients with reperfused ST-elevation myocardial infarction. J Cardiovasc Magn Reson. 2016;18:80.

83. Khan JN, Nazir SA, Greenwood JP, et al. Infarct size following complete revascularization in patients presenting with STEMI: a comparison of immediate and staged in-hospital non-infarct related artery PCI subgroups in the CvLPRIT study. J Cardiovasc Magn Reson. 2016;18:85.

84. Papanastasiou G, Williams MC, Dweck MR, et al. Quantitative assessment of myocardial blood flow in coronary artery disease by cardiovascular magnetic resonance: comparison of Fermi and distributed parameter modeling against invasive methods. J Cardiovasc Magn Reson. 2016;18:57.

85. Cardona M, Martin V, Prat-Gonzalez S, et al. Benefits of chronic total coronary occlusion percutaneous intervention in patients with heart failure and reduced ejection fraction: insights from a cardiovascular magnetic resonance study. J Cardiovasc Magn Reson. 2016;18:78.

86. Stromp TA, Leung SW, Andres KN, Jing L, Fornwalt BK, Charnigo RJ, Sorrell VL, Vandsburger MH. Gadolinium free cardiovascular magnetic resonance with 2-point cine balanced steady state free precession. J Cardiovasc Magn Reson. 2015;17:90.

87. Edelman RR, Giri S, Pursnani A, Botelho MP, Li W, Koktzoglou I. Breath-hold imaging of the coronary arteries using quiescent-interval slice-selective (QISS) magnetic resonance angiography: pilot study at 1.5 Tesla and 3 Tesla. J Cardiovasc Magn Reson. 2015;17:101.

88. Basar B, Rogers T, Ratnayaka K, Campbell-Washburn AE, Mazal JR, Schenke WH, Sonmez M, Faranesh AZ, Lederman RJ, Kocaturk O. Segmented nitinol guidewires with stiffness-matched connectors for cardiovascular magnetic resonance catheterization: preserved mechanical performance and freedom from heating. J Cardiovasc Magn Reson. 2015;17:105.

89. Vardoulis O, Monney P, Bermano A, Vaxman A, Gotsman C, Schwitter J, Stuber M, Stergiopoulos N, Schwitter J. Single breath-hold 3D measurement of left atrial volume using compressed sensing cardiovascular magnetic resonance and a non-model-based reconstruction approach. J Cardiovasc Magn Reson. 2015;17:47.

90. Chow K, Kellman P, Spottiswoode BS, Nielles-Vallespin S, Arai AE, Salerno M, Thompson RB. Saturation pulse design for quantitative myocardial T1 mapping. J Cardiovasc Magn Reson. 2015;17:84.

91. Xanthis CG, Bidhult S, Kantasis G, Heiberg E, Arheden H, Aletras AH. Parallel simulations for QUAntifying RElaxation magnetic resonance constants (SQUAREMR): an example towards accurate MOLLI T1 measurements. J Cardiovasc Magn Reson. 2015;17:104.

92. Mahmod M, Piechnik SK, Levelt E, Ferreira VM, Francis JM, Lewis A, Pal N, Dass S, Ashrafian H, Neubauer S, Karamitsos TD. Adenosine stress native T1 mapping in severe aortic stenosis: evidence for a role of the intravascular compartment on myocardial T1 values. J Cardiovasc Magn Reson. 2014;16:92.

93. McDiarmid AK, Swoboda PP, Erhayiem B, Ripley DP, Kidambi A, Broadbent DA, Higgins DM, Greenwood JP, Plein S. Single bolus versus split dose gadolinium administration in extra-cellular volume calculation at 3 Tesla. J Cardiovasc Magn Reson. 2015;17:6.

94. Kellman P, Bandettini WP, Mancini C, Hammer-Hansen S, Hansen MS, Arai AE. Characterization of myocardial T1-mapping bias caused by intramyocardial fat in inversion recovery and saturation recovery techniques. J Cardiovasc Magn Reson. 2015;17:33.

95. Treibel TA, Zemrak F, Sado DM, Banypersad SM, White SK, Maestrini V, Barison A, Patel V, Herrey AS, Davies C, Caulfield MJ, Petersen SE, Moon JC. Extracellular volume quantification in isolated hypertension - changes at the detectable limits? J Cardiovasc Magn Reson. 2015;17:74.

96. Ertel A, Pratt D, Kellman P, Leung S, Bandettini P, Long LM, Young M, Nelson C, Arai AE, Druey KM. Increased myocardial extracellular volume in active idiopathic systemic capillary leak syndrome. J Cardiovasc Magn Reson. 2015;17:76.

97. de Meester de Ravenstein C, Bouzin C, Lazam S, Boulif J, Amzulescu M, Melchior J, Pasquet A, Vancraeynest D, Pouleur AC, Vanoverschelde JLJ, Gerber BL. Histological validation of measurement of diffuse interstitial myocardial fibrosis by myocardial extravascular volume fraction from modified look-locker imaging (MOLLI) T1 mapping at 3T. J Cardiovasc Magn Reson. 2015;17:48.

98. Baeßler B, Schaarschmidt F, Stehning C, Schnackenburg B, Maintz D, Bunck AC. Cardiac T2-mapping using a fast gradient echo spin echo sequence - first in vitro and in vivo experience. J Cardiovasc Magn Reson. 2015;17:67.

99. Sprinkart AM, Luetkens JA, Träber F, Doerner J, Gieseke J, Schnackenburg B, Schmitz G, Thomas D, Homsi R, Block W, Schild H, Naehle CP. Gradient spin Echo (GraSE) imaging for fast myocardial T2 mapping. J Cardiovasc Magn Reson. 2015;17:12.

100. Bönner F, Janzarik N, Jacoby C, Spieker M, Schnackenburg B, Range F, Butzbach B, Haberkorn S, Westenfeld R, Neizel-Wittke M, Flögel U, Kelm M. Myocardial T2 mapping reveals age- and sex-related differences in volunteers. J Cardiovasc Magn Reson. 2015;17:9.

101. Baeßler B, Schaarschmidt F, Dick A, Stehning C, Schnackenburg B, Michels G, Maintz D, Bunck AC. Mapping tissue inhomogeneity in acute myocarditis: a novel analytical approach to quantitative myocardial edema imaging by T2-mapping. J Cardiovasc Magn Reson. 2015;17:115.

102. Hagio T, Huang C, Abidov A, Singh J, Ainapurapu B, Squire S, Bruck D, Altbach MI. T 2 mapping of the heart with a double-inversion radial fast

spin-echo method with indirect echo compensation. J Cardiovasc Magn Reson. 2015;17:24.

103. Jin N, da Silveira JS, Jolly MP, Firmin DN, Mathew G, Lamba N, Subramanian S, Pennell DJ, Raman SV, Simonetti OP. Free-breathing myocardial T2* mapping using GRE-EPI and automatic non-rigid motion correction. J Cardiovasc Magn Reson. 2015;17:113.

104. Sandino CM, Kellman P, Arai AE, Hansen MS, Xue H. Myocardial T2* mapping: influence of noise on accuracy and precision. J Cardiovasc Magn Reson. 2015;17:7.

105. Contijoch F, Witschey WRT, Rogers K, Rears H, Hansen M, Yushkevich P, Gorman J, Gorman RC, Han Y. User-initialized active contour segmentation and golden-angle real-time cardiovascular magnetic resonance enable accurate assessment of LV function in patients with sinus rhythm and arrhythmias. J Cardiovasc Magn Reson. 2015;17:37.

106. Roujol S, Basha TA, Weingärtner S, Akçakaya M, Berg S, Manning WJ, Nezafat R. Impact of motion correction on reproducibility and spatial variability of quantitative myocardial T2 mapping. J Cardiovasc Magn Reson. 2015;17:46.

107. Stirrat J, Joncas SX, Salerno M, Drangova M, White J. Influence of phase correction of late gadolinium enhancement images on scar signal quantification in patients with ischemic and non-ischemic cardiomyopathy. J Cardiovasc Magn Reson. 2015;17:66.

108. Ferreira VM, Wijesurendra RS, Liu A, Greiser A, Casadei B, Robson MD, Neubauer S, Piechnik SK. Systolic ShMOLLI myocardial T1-mapping for improved robustness to partial-volume effects and applications in tachyarrhythmias. J Cardiovasc Magn Reson. 2015;17:77.

109. Kellman P, Xue H, Spottiswoode BS, Sandino CM, Hansen MS, Abdel-Gadir A, Treibel TA, Rosmini S, Mancini C, Bandettini WP, McGill LA, Gatehouse P, Moon JC, Pennell DJ, Arai AE. Free-breathing T2* mapping using respiratory motion corrected averaging. J Cardiovasc Magn Reson. 2015;17:3.

110. Krishnamurthy R, Pednekar A, Atweh LA, Vogelius E, Chu ZD, Zhang W, Maskatia S, Masand P, Morris SA, Krishnamurthy R, Muthupillai R. Clinical validation of free breathing respiratory triggered retrospectively cardiac gated cine balanced steady-state free precession cardiovascular magnetic resonance in sedated children. J Cardiovasc Magn Reson. 2015;17:1.

111. Wehner GJ, Suever JD, Haggerty CM, Jing L, Powell DK, Hamlet SM, Grabau JD, Mojsejenko WD, Zhong X, Epstein FH, Fornwalt BK. Validation of in vivo 2D displacements from spiral cine DENSE at 3T. J Cardiovasc Magn Reson. 2015;17:5.

112. Brink WM, van den Brink JS, Webb AG. The effect of high-permittivity pads on specific absorption rate in radiofrequency-shimmed dual-transmit cardiovascular magnetic resonance at 3T. J Cardiovasc Magn Reson. 2015;17:82.

113. Miller CA, Hsu LY, Ta A, Conn H, Winkler S, Arai AE. Quantitative pixel-wise measurement of myocardial blood flow. The impact of surface coil-related field inhomogeneity and a comparison of methods for its correction. J Cardiovasc Magn Reson. 2015;17:11.

114. Nayak KS, Nielsen JF, Bernstein MA, Markl M, Gatehouse PD, Botnar RM, Saloner D, Lorenz C, Wen H, Hu BS, Epstein FH, Oshinski JN, Raman SV. Cardiovascular magnetic resonance phase contrast imaging. J Cardiovasc Magn Reson. 2015;17:71.

115. Keegan J, Raphael CE, Parker K, Simpson RM, Strain S, de Silva R, Di Mario C, Collinson J, Stables RH, Wage R, Drivas P, Sugathapala M, Prasad SK, Firmin DN. Validation of high temporal resolution spiral phase velocity mapping of temporal patterns of left and right coronary artery blood flow against Doppler guidewire. J Cardiovasc Magn Reson. 2015;17:85.

116. Motwani M, Kidambi A, Uddin A, Sourbron S, Greenwood JP, Plein S. Quantification of myocardial blood flow with cardiovascular magnetic resonance throughout the cardiac cycle. J Cardiovasc Magn Reson. 2015;17:4.

117. Tsai-Goodman B, Zhu MY, Al-Rujaib M, Seed M, Macgowan CK. Foetal blood flow measured using phase contrast cardiovascular magnetic resonance - preliminary data comparing 1.5T with 3.0T. J Cardiovasc Magn Reson. 2015;17:30.

118. Dyverfeldt P, Bissell M, Barker AJ, Bolger AF, Carlhäll CJ, Ebbers T, Francios CJ, Frydrychowicz A, Geiger J, Giese D, Hope MD, Kilner PJ, Kozerke S, Myerson S, Neubauer S, Wieben O, Markl M. 4D flow cardiovascular magnetic resonance consensus statement. J Cardiovasc Magn Reson. 2015;17:72.

119. Bustamante M, Petersson S, Eriksson J, Alehagen U, Dyverfeldt P, Carlhäll CJ, Ebbers T. Atlas-based analysis of 4D flow CMR: automated vessel segmentation and flow quantification. J Cardiovasc Magn Reson. 2015;17:87.

120. Kanski M, Arvidsson PM, Töger J, Borgquist R, Heiberg E, Carlsson M, Arheden H. Left ventricular fluid kinetic energy time curves in heart failure from cardiovascular magnetic resonance 4D flow data. J Cardiovasc Magn Reson. 2015;17:111.

121. Nielles-Vallespin S, Kellman P, Hsu LY, Arai AE. FLASH proton density imaging for improved surface coil intensity correction in quantitative and semi-quantitative SSFP perfusion cardiovascular magnetic resonance. J Cardiovasc Magn Reson. 2015;17:16.

122. Sammut E, Zarinabad N, Wesolowski R, Morton G, Chen Z, Sohal M, Carr-White G, Razavi R, Chiribiri A. Feasibility of high-resolution quantitative perfusion analysis in patients with heart failure. J Cardiovasc Magn Reson. 2015;17:13.

123. Andre F, Steen H, Matheis P, Westkott M, Breuninger K, Sander Y, Kammerer R, Galuschky C, Giannitsis E, Korosoglou G, Katus HA, Buss SJ. Age- and genderrelated normal left ventricular deformation assessed by cardiovascular magnetic resonance feature tracking. J Cardiovasc Magn Reson. 2015;17:25.

124. Kihlberg J, Haraldsson H, Sigfridsson A, Ebbers T, Engvall JE. Clinical experience of strain imaging using DENSE for detecting infarcted cardiac segments. J Cardiovasc Magn Reson. 2015;17:50.

125. Dibb R, Qi Y, Liu C. Magnetic susceptibility anisotropy of myocardium imaged by cardiovascular magnetic resonance reflects the anisotropy of myocardial filament alpha-helix polypeptide bonds. J Cardiovasc Magn Reson. 2015;17:60.

126. Wehner GJ, Grabau JD, Suever JD, Haggerty CM, Jing L, Powell DK, Hamlet SM, Vandsburger MH, Zhong X, Fornwalt BK. 2D cine DENSE with low encoding frequencies accurately quantifies cardiac mechanics with improved image characteristics. J Cardiovasc Magn Reson. 2015;17:93.

127. Likhite D, Adluru G, Hu N, McGann C, DiBella E. Quantification of myocardial perfusion with self-gated cardiovascular magnetic resonance. J Cardiovasc Magn Reson. 2015;17:14.

128. Papanastasiou G, Williams MC, Kershaw LE, Dweck MR, Alam S, Mirsadraee S, Connell M, Gray C, MacGillivray T, Newby DE, Semple SI. Measurement of myocardial blood flow by cardiovascular magnetic resonance perfusion: comparison of distributed parameter and Fermi models with single and dual bolus. J Cardiovasc Magn Reson. 2015;17:17.

129. Sánchez-González J, Fernandez-Jiménez R, Nothnagel ND, López-Martín G, Fuster V, Ibañez B. Optimization of dual-saturation single bolus acquisition for quantitative cardiac perfusion and myocardial blood flow maps. J Cardiovasc Magn Reson. 2015;17:21.

130. Wissmann L, Niemann M, Gotschy A, Manka R, Kozerke S. Quantitative three-dimensional myocardial perfusion cardiovascular magnetic resonance with accurate two-dimensional arterial input function assessment. J Cardiovasc Magn Reson. 2015;17:108.

131. Parnham S, Gleadle JM, Leong D, Grover S, Bradbrook C, Woodman RJ, De Pasquale CG, Selvanayagam JB. Myocardial perfusion is impaired in asymptomatic renal and liver transplant recipients: a cardiovascular magnetic resonance study. J Cardiovasc Magn Reson. 2015;17:56.

132. Fair MJ, Gatehouse PD, DiBella EV, Firmin DN. A review of 3D first-pass, whole-heart, myocardial perfusion cardiovascular magnetic resonance. J Cardiovasc Magn Reson. 2015;17:68.

133. Riffel JH, Andre F, Maertens M, Rost F, Keller MGP, Giusca S, Seitz S, Kristen AV, Müller M, Giannitsis E, Korosoglou G, Katus HA, Buss SJ. Fast assessment of long axis strain with standard cardiovascular magnetic resonance: a validation study of a novel parameter with reference values. J Cardiovasc Magn Reson. 2015;17:69.

134. Bernus O, Radjenovic A, Trew ML, LeGrice IJ, Sands GB, Magee DR, Smaill BH, Gilbert SH. Comparison of diffusion tensor imaging by cardiovascular magnetic resonance and gadolinium enhanced 3D image intensity approaches to investigation of structural anisotropy in explanted rat hearts. J Cardiovasc Magn Reson. 2015;17:31.

135. Okafor IU, Santhanakrishnan A, Chaffins BD, Mirabella L, Oshinski JN, Yoganathan AP. Cardiovascular magnetic resonance compatible physical model of the left ventricle for multi-modality characterization of wall motion and hemodynamics. J Cardiovasc Magn Reson. 2015;17:51.

136. Cross R, Olivieri L, O'Brien K, et al. Improved workflow for quantification of left ventricular volumes and mass using free-breathing motion corrected cine imaging. J Cardiovasc Magn Reson. 2016;18:10.

137. Zhao L, Li S, Ma X, et al. Systolic MOLLI T1 mapping with heart-rate dependent pulse sequence sampling scheme is feasible in patients with atrial fibrillation. J Cardiovasc Magn Reson. 2016;18:13.

138. Jacobs M, Benovoy M, Chang LC, et al. Evaluation of an automated method for arterial input function detection for first pass myocardial perfusion cardiovascular magnetic resonance. J Cardiovasc Magn Reson. 2016;18:17.

139. Alam MH, He T, Auger D, et al. Validation of T2* in-line analysis for tissue iron quantification at 1.5T. J Cardiovasc Magn Reson. 2016;18:23.

140. Kuetting DL, Dabir D, Homsi DR, et al. The effects of extracellular contrast agent (gadobutrol) on the precision and reproducibility of cardiovascular magnetic resonance feature tracking. J Cardiovasc Magn Reson. 2016;18:30.

141. Chen X, Yang Y, Cai X, et al. Accelerated two-dimensional cine DENSE cardiovascular magnetic resonance using compressed sensing and parallel imaging. J Cardiovasc Magn Reson. 2016;18:38.

142. Alam MH, Auger D, McGill LA, et al. Comparison of 3T and 1.5T for T2* magnetic resonance of tissue iron. J Cardiovasc Magn Reson. 2016;18:40.

143. Guensch DP, Nadeshalingam G, Fischer K, et al. The impact of hematocrit on oxygenation-sensitive cardiovascular magnetic resonance. J Cardiovasc Magn Reson. 2016;18:42.

144. Stirrat CG, Alam SR, MacGiollivray TJ, et al. Ferumoxytol-enhanced magnetic resonance imaging methodology and normal values at 1.5T and 3T. J Cardiovasc Magn Reson. 2016;18:46.

145. Chow K, Yang Y, Shaw P, et al. Robust free-breathing SASHA T1 mapping with high-contrast image registration. J Cardiovasc Magn Reson. 2016;18:47.

146. Kido T, Kido T, Nakamura M, et al. Compressed sensing real-time cine cardiovascular magnetic resonance: accurate assessment of left ventricular function in a single breath-hold. J Cardiovasc Magn Reson. 2016;18:50.

147. Hamlet SM, Haggerty CM, Suever JD, et al. An interactive videogame designed to improve respiratory navigator efficiency in children undergoing cardiovascular magnetic resonance. J Cardiovasc Magn Reson. 2016;18:54.

148. Bertelsen L, Svendsen JH, Lober L, et al. Flow measurement at the aortic root – impact of location of through-plane phase contrast velocity mapping. J Cardiovasc Magn Reson. 2016;18:55.

149. Captur G, Gatehouse P, Keenan KE, et al. A medical device-grade T1 and ECV phantom for global T1 mapping quality assurance – the T1 mapping and ECV standardization in cardiovascular magnetic resonance (T1MES) program. J Cardiovasc Magn Reson. 2016;18:58.

150. Jarvis K, Vonder M, Barker AJ, et al. Hemodynamic evaluation in patients with transposition of the great arteries after the arterial switch operation: 4D flow and 2D phase contrast cardiovascular magnetic resonance compared with Doppler echocardiography. J Cardiovasc Magn Reson. 2016;18:59.

151. D'Errico L, Lamacie MM, Juan LJ, et al. Effects of slice orientation on reproducibility of sequential assessment of right ventricular volumes and ejection fraction: short-axis vs. transverse SSFP cine cardiovascular magnetic resonance. J Cardiovasc Magn Reson. 2016;18:60.

152. Vassilou VS, GHeng EL, Gatehouse PD, et al. Magnetic resonance imaging phantoms for quality-control of myocardial T1 and ECV mapping: specific formulation, long-term stability and variation with heart rate and temperature. J Cardiovasc Magn Reson. 2016;18:62.

153. Tandon A, James L, Henningsson M, et al. A clinical combined gadobutrol bolus and slow infusion protocol enabling angiography, inversion recovery whole heart, and late gadolinium enhancement imaging in a single study. J Cardiovasc Magn Reson. 2016;18:66.

154. Edelman RR, Botelho M, Pursnani A, et al. Improved dark blood imaging of the heart using radial balanced steady state free precession. J Cardiovasc Magn Reson. 2016;18:69.

155. Kellman P, Xue H, Olivieri LJ, et al. Dark blood late gadolinium enhancement. J Cardiovasc Magn Reson. 2016;18:77.

156. Raphael CE, Keegan J, Parker KH, et al. Feasibility of cardiovascular magnetic resonance derived coronary wave intensity analysis. J Cardiovasc Magn Reson. 2016;18:93.

157. McGill LA, Ferreira PF, Scott AD, et al. Relationship between cardiac diffusion tensor imaging parameters and anthropometrics in healthy volunteers. J Cardiovasc Magn Reson. 2016;18:2.

158. Opriessnig P, Mangge H, Stollberger R, et al. In vivo cardiovascular magnetic resonance of 2D vessel wall diffusion anisotropy in carotid arteries. J Cardiovasc Magn Reson. 2016;18:81.

159. Zhou Z, Li R, Zhao X, He L, Wang X, Wang J, Balu N, Yuan C. Evaluation of 3D multi-contrast joint intra- and extracranial vessel wall cardiovascular magnetic resonance. J Cardiovasc Magn Reson. 2015;17:41.

160. Alam SR, Stirrat C, Richards J, Mirsadraee S, Semple SI, Tse G, Henriksen P, Newby DE. Vascular and plaque imaging with ultrasmall superparamagnetic particles of iron oxide. J Cardiovasc Magn Reson. 2015;17:83.

161. van den Bosch HCM, Westenberg JJM, Setz-Pels W, Wondergem J, Wolterbeek R, Duijm LEM, Teijink JAW, de Roos A. Site-specific association between distal aortic pulse wave velocity and peripheral arterial stenosis severity: a prospective cardiovascular magnetic resonance study. J Cardiovasc Magn Reson. 2015;17:2.

162. Keegan J, Patel HC, Simpson RM, Mohiaddin RH, Firmin DN. Inter-study reproducibility of interleaved spiral phase velocity mapping of renal artery haemodynamics. J Cardiovasc Magn Reson. 2015;17:8.

163. Langham MC, Zhou Y, Chirico EN, Magland JF, Sehgal CM, Englund EK, Mohler ER, Guo W, Barhoum S, Wehrli FW. Effects of age and smoking on endothelial function assessed by quantitative cardiovascular magnetic resonance in the peripheral and central vasculature. J Cardiovasc Magn Reson. 2015;17:19.

164. Nethononda RM, Lewandowski AJ, Stewart R, Kylinterias I, Whitworth P, Francis J, Leeson P, Watkins H, Neubauer S, Rider OJ. Gender specific patterns of age-related decline in aortic stiffness: a cardiovascular magnetic resonance study including normal ranges. J Cardiovasc Magn Reson. 2015;17:20.

165. Bargiotas I, Mousseaux E, Yu WC, Venkatesh BA, Bollache E, de Cesare A, Lima JAC, Redheuil A, Kachenoura N. Estimation of aortic pulse wave transit time in cardiovascular magnetic resonance using complex wavelet crossspectrum analysis. J Cardiovasc Magn Reson. 2015;17:65.

166. Roberts PA, Cowan BR, Liu Y, Lin AC, Nielsen PM, Taberner AJ, Stewart RA, Lam HI, Young AA. Real-time aortic pulse wave velocity measurement during exercise stress testing. J Cardiovasc Magn Reson. 2015;17:86.

167. Forouzan O, Warczytowa J, Wieben O, François CJ, Chesler NC. Non-invasive measurement using cardiovascular magnetic resonance of changes in pulmonary artery stiffness with exercise. J Cardiovasc Magn Reson. 2015;17:109.

168. Steeden JA, Pandya B, Tann O, Muthurangu V. Free breathing contrastenhanced time-resolved magnetic resonance angiography in pediatric and adult congenital heart disease. J Cardiovasc Magn Reson. 2015;17:38.

169. Lopez D, Pollak AW, Meyer CH, Epstein FH, Zhao L, Pesch AJ, Jiji R, Kay JR, DiMaria JM, Christopher JM, Kramer CM. Arterial spin labeling perfusion cardiovascular magnetic resonance of the calf in peripheral arterial disease: cuff occlusion hyperemia vs exercise. J Cardiovasc Magn Reson. 2015;17:23.

170. Saam T, Habs M, Buchholz M, et al. Expansive arterial remodeling of the carotid arteries and its effect on atherosclerotic plaque composition and vulnerability: an in-vivo black-blood 3T CMR study in symptomatic stroke patients. J Cardiovasc Magn Reson. 2016;18:11.

171. Kokzoglou I, Walker MT, Meyer JR, et al. Nonenhanced hybridized arterial spin labeled magnetic resonance angiography of the extracranial carotid arteries using a fast low angle shot readout at 3 Tesla. J Cardiovasc Magn Reson. 2016;18:18.

172. Al Musa T, Uddin A, Fairbairn TA, et al. Assessment of aortic stiffness by cardiovascular magnetic resonance following the treatment of severe aortic stenosis by TAVI and surgical AVR. J Cardiovasc Magn Reson. 2016;18:37.

173. Liu J, Balu N, Hippe DS, et al. Semi-automatic carotid intraplaque hemorrhage detection and quantification on magnetization-prepared rapid acquisition gradient-Echo (MP-RAGE) with optimized threshold selection. J Cardiovasc Magn Reson. 2016;18:41.

174. Voges I, Kees J, Jerosch-Herold M, et al. Aortic stiffness and its impact on left atrial volumes and function in patients after successful coarctation repair: a multiparametric cardiovascular magnetic resonance study. J Cardiovasc Magn Reson. 2016;18:56.

175. Wu G, Yang J, Zhang T, et al. The diagnostic value of non-contrast enhanced quiescent interval single shot (QISS) magnetic resonance angiography at 3T for lower extremity peripheral arterial disease, in comparison to CT angiography. J Cardiovasc Magn Reson. 2016;18:71.

176. Tandon A, Hashemi S, Parks WJ, et al. Improved high-resolution pediatric vascular cardiovascular magnetic resonance with gadofosveset-enhanced 3D respiratory navigated, inversion recovery prepared gradient echo readout imaging compared to 3D balanced steady-state free precession readout imaging. J Cardiovasc Magn Reson. 2016;18:74.

177. Xu Y, Yuan C, Zhou Z, et al. Co-existing intracranial and extracranial carotid artery atherosclerosis plaques and recurrent stroke risk: a three-dimensional multicontrast cardiovascular magnetic resonance study. J Cardiovasc Magn Reson. 2016;18:90.

178. Abdesselam I, Pepino P, Troalen T, Macia M, Ancel P, Masi B, Fourny N, Gaborit B, Giannesini B, Kober F, Dutour A, Bernard M. Time course of

cardiometabolic alterations in a high fat high sucrose diet mice model and improvement after GLP-1 analog treatment using multimodal cardiovascular magnetic resonance. J Cardiovasc Magn Reson. 2015;17:95.

179. Maguire ML, Geethanath S, Lygate CA, Kodibagkar VD, Schneider JE. Compressed sensing to accelerate magnetic resonance spectroscopic imaging: evaluation and application to 23Na-imaging of mouse hearts. J Cardiovasc Magn Reson. 2015;17:45.

180. Schär M, Gabr RE, El-Sharkawy AM, Steinberg A, Bottomley PA, Weiss RG. Two repetition time saturation transfer (TwiST) with spill-over correction to measure creatine kinase reaction rates in human hearts. J Cardiovasc Magn Reson. 2015;17:70.

181. Haggerty CM, Mattingly AC, Kramer SP, Binkley CM, Jing L, Suever JD, Powell DK, Charnigo RJ, Epstein FH, Fornwalt BK. Left ventricular mechanical dysfunction in diet-induced obese mice is exacerbated during inotropic stress: a cine DENSE cardiovascular magnetic resonance study. J Cardiovasc Magn Reson. 2015;17:75.

182. Trotier AJ, Lefrançois W, Van Renterghem K, Franconi JM, Thiaudière E, Miraux S. Positive contrast high-resolution 3D-cine imaging of the cardiovascular system in small animals using a UTE sequence and iron nanoparticles at 4.7, 7 and 9.4T. J Cardiovasc Magn Reson. 2015;17:53.

183. Fernández-Jiménez R, Sánchez-González J, Aguero J, Del Trigo M, Galán-Arriola C, Fuster V, Ibáñez B. Fast T2 gradient-spin-echo (T2-GraSE) mapping for myocardial edema quantification: first in vivo validation in a porcine model of ischemia/reperfusion. J Cardiovasc Magn Reson. 2015;17:92.

184. Thomas RM, Lim SY, Qiang B, Osherov AB, Ghugre NR, Noyan H, Qi X, Wolff R, Ladouceur-Wodzak M, Berk TA, Butany J, Husain M, Wright GA, Strauss BH. Distal coronary embolization following acute myocardial infarction increases early infarct size and late left ventricular wall thinning in a porcine model. J Cardiovasc Magn Reson. 2015;17:106.

185. Azene N, Fu Y, Maurer J, Kraitchman DL. Tracking of stem cells in vivo for cardiovascular applications. J Cardiovasc Magn Reson. 2014;16:7.

186. Jeuthe S, Wassilew AK, Oh-Ici DO, et al. Myocardial T1 maps reflect histological findings in acute and chronic stages of myocarditis in a rat model. J Cardiovasc Magn Reson. 2016;18:19.

187. Engblom H, Tufvesson J, Joblonowski R, et al. A new automatic algorithm for quantification of myocardial infarction imaged by late gadolinium enhancement cardiovascular magnetic resonance: experimental validation and comparison to expert delineations in multi-center, multi-vendor patient data. J Cardiovasc Magn Reson. 2016;18:27.

188. Naresh NK, Butcher JT, Lye RJ, et al. Cardiovascular magnetic resonance detectgs the progression of impaired myocardial perfusion reserve and increased left-ventricular mass in mice fed a high-fat diet. J Cardiovasc Magn Reson. 2016;18:53.

189. Reiter U, Reiter G, Manninger M, et al. Early-stage heart failure with preserved ejection fraction in the pig: a cardiovascular magnetic resonance study. J Cardiovasc Magn Reson. 2016;18:63.

190. Lu JC, Nielsen JC, Morowitz L, Musani M, Mahani MG, Agarwal PP. Ibrahim el-SH, Dorfman AL. Use of a 1.0 Tesla open scanner for evaluation of pediatric and congenital heart disease: a retrospective cohort study. J Cardiovasc Magn Reson. 2015;17:39.

191. Pushparajah K, Tzifa A, Bell A, Wong JK, Hussain T, Valverde I, Bellsham-nnRevell HR, Greil G, Simpson JM, Schaeffter T, Razavi R. Cardiovascular magnetic resonance catheterization derived pulmonary vascular resistance and medium-term outcomes in congenital heart disease. J Cardiovasc Magn Reson. 2015;17:28.

192. Truong U, Patel S, Kheyfets V, Dunning J, Fonseca B, Barker AJ, Ivy D, Shandas R, Hunter K. Non-invasive determination by cardiovascular magnetic resonance of right ventricular-vascular coupling in children and adolescents with pulmonary hypertension. J Cardiovasc Magn Reson. 2015;17:81.

193. Monney P, Piccini D, Rutz T, Vincenti G, Coppo S, Koestner SC, Sekarski N, Di Bernardo S, Bouchardy J, Stuber M, Schwitter J. Single centre experience of the application of self navigated 3D whole heart cardiovascular magnetic resonance for the assessment of cardiac anatomy in congenital heart disease. J Cardiovasc Magn Reson. 2015;17:55.

194. Monney P, Piccini D, Rutz T, Vincenti G, Coppo S, Koestner SC, Sekarski N, Di Bernardo S, Bouchardy J, Stuber M, Schwitter J. Erratum to: single centre experience of the application of self-navigated 3D whole heart cardiovascular magnetic resonance for the assessment of cardiac anatomy in congenital heart disease. J Cardiovasc Magn Reson. 2015;17:88.

195. Calkoen EE, Westenberg JJM, Kroft LJM, Blom NA, Hazekamp MG, Rijlaarsdam ME, Jongbloed MRM, de Roos A, Roest AAW. Characterization and quantification of dynamic eccentric regurgitation of the left atrioventricular valve after atrioventricular septal defect correction with 4D flow cardiovascular magnetic resonance and retrospective valve tracking. J Cardiovasc Magn Reson. 2015;17:18.

196. Kato A, Drolet C, Yoo SJ, et al. Vicious circle between progressive right ventricular dilation and pulmonary regurgitation in patients after tetralogy of fallow repair. Right heart enlargement promotes flow reversal in the left pulmonary artery. J Cardiovasc Magn Reson. 2016;18:34.

197. Jing L, Wehner GJ, Suever JD, et al. Left and right ventricular dyssynchrony and strains from cardiovascular magnetic resonance feature tracking do not predict deterioration of ventricular function in patients with repaired tetralogy of Fallot. J Cardiovasc Magn Reson. 2016;18:49.

198. Riesenkampff E, Luining W, Seed M, et al. Increased left ventricular myocardial extracellular volume is associated with longer cardiopulmonary bypass times, biventricular enlargement and reduced exercise tolerance in children after repair of Tetralogy of Fallot. J Cardiovasc Magn Reson. 2016;18:75.

199. Crouch G, Tully PJ, Bennetts J, Sinhal A, Bradbrook C, Penhall AL, De Pasquale CG, Baker RA, Selvanayagam JB. Quantitative assessment of paravalvular regurgitation following transcatheter aortic valve replacement. J Cardiovasc Magn Reson. 2015;17:32.

200. Captur G, Karperien AL, Li C, Zemrak F, Tobon-Gomez C, Gao X, Bluemke DA, Elliott PM, Petersen SE, Moon JC. Fractal frontiers in cardiovascular magnetic resonance: towards clinical implementation. J Cardiovasc Magn Reson. 2015;17:80.

201. Keller EJ, Vogelzang RL, Freed BH, Carr JC, Collins JD. Physician's professional identities: a roadmap to understanding "value" in cardiovascular imaging. J Cardiovasc Magn Reson. 2016;18:52.

202. Piekarski E, Chitiboi T, Ramb R, Feng L, Axel L. Use of self-gated radial cardiovascular magnetic resonance to detect and classify arrhythmias (atrial fibrillation and premature ventricular contraction). J Cardiovasc Magn Reson. 2016;18:83.

203. Khan MS, Ullah W, Riaz IB, et al. Top 100 cited articles in cardiovascular magnetic resonance: a bibliometric analysis. J Cardiovasc Magn Reson. 2016;18:87.

204. Liao PA, Lin G, Tsai SY, et al. Myocardial triglyceride content at 3T cardiovascular magnetic resonance and left ventricular systolic function: a cross-sectional study in patients hospitalized with acute heart failure. J Cardiovasc Magn Reson. 2016;18:9.

205. Kober F, Jao T, Troalen T, Nayak KS. Myocardial arterial spin labeling. J Cardiovasc Magn Reson. 2016;18:22.

206. Rodrigues JCL, Lyen SM, Loughborough W, et al. Extra-cardiac findings in cardiovascular magnetic resonance: what the imaging cardiologist needs to know. J Cardiovasc Magn Reson. 2016;18:26.

207. Pedrizzetti G, Claus P, Killner PJ, Nagel E. Principles of cardiovascular magnetic resonance feature tracking and echocardiographic speckle tracking for informed clinical use. J Cardiovasc Magn Reson. 2016;18:51.

208. Placido R, Lopes BC, Almeida AG, Rochitte CE. The role of cardiovascular magnetic resonance in Takotsubo syndrome. J Cardiovasc Magn Reson. 2016;18:68.

209. Haaf P, Garg P, Messroghli DR, et al. Cardiac T1 mapping and extracellular volume (ECV) in clinical practice: a comprehensive review. J Cardiovasc Magn Reson. 2016;18:89.

210. Abdel-Gadir A, Berber R, Porter JB, et al. Detection of metallic cobalt and chromium liver deposition followed failed hip replacement using T2* and R2 magnetic resonance. J Cardiovasc Magn Reson. 2016;18:29.